A Thorough Study on the Relationships Between Dispersion Quality and Viscoelastic Properties in Carbon Black Filled SBR Compounds

Jean L. Leblanc,[1] Matthew Putman,[2] Ekkawit Pianhanuruk[3]

[1]*UPMC Paris-Sorbonne University, Polymer Rheology and Processing, Vitry-sur-Seine, France*
[2]*Department of Applied Physics and Mathematics, Columbia University, New York*
[3]*Université du Maine, UCO2M UMR CNRS 6011, Le Mans, France*

Received 30 June 2010; accepted 22 November 2010
DOI 10.1002/app.33793
Published online 25 February 2011 in Wiley Online Library (wileyonlinelibrary.com).

ABSTRACT: A series of carbon black filled SBR 1500 compounds (without curatives) were prepared in carefully controlled lab-mixing conditions so that filler content ranged from 0 to 50 phr, with the usual compounding ingredients. Carbon Black agglomeration and dispersion quality were assessed through an advanced microscopic technique with automated data treatment. Linear and nonlinear viscoelastic properties were evaluated using a closed cavity torsional rheometer, equipped for Fourier Transform rheometry experiments. In the linear viscoelastic regime, dynamic moduli mastercurves were derived from experiments in the 60−160°C temperature range. In the nonlinear viscoelastic regime, complex modulus and torque harmonics variation with strain amplitude were investigated at 100°C and frequency 0.5 and 1.0 Hz. Relationships between dispersion quality, carbon black loading and mixing parameters were investigated so that dispersion appears better when the filler loading is above a critical level that to some extent (but not exactly) corresponds to the theoretical percolation threshold (around 13%). Linear and nonlinear viscoelastic measurements demonstrate and quantify the role played by plasticizing compounding ingredients, that is, processing oil, stearic acid and other chemicals, with nearly no significant effect of mixing energy. At least 10−15 phr carbon black are necessary to recover the modulus loss associated with this plasticizing effect. Nonlinear results and particularly the torque harmonics reveal a number of details as to how the compounding ingredients do affect the viscoelastic behavior, with expectedly the carbon black playing the major role. By fitting results with mathematically simple models, all of the observed effects can be summarized in a rather limited number of parameters so that the effects of compounding ingredients can be studied in details. © 2011 Wiley Periodicals, Inc. J Appl Polym Sci 121: 1096–1117, 2011

Key words: rubber; carbon black; viscoelastic properties; compounding; modeling

INTRODUCTION

Complex polymer systems such as carbon black filled rubber compounds exhibit specific properties whose origin is currently assigned to interactions occurring between the rubber matrix and the filler particles, and the associated self-structuring that results from such interactions. Numerous engineering applications pragmatically use those specificities but, despite near a century of successful development, there are still a number of obscure points that are worth considering. From a fundamental point of view, one can see such systems as multiple layers of reduction to fully comprehend and model the physical behavior of the involved microstructures and macrostructures. Theories that take into account classical hydrodynamics, rupture mechanics, percolation concept, and many tools developed in rheology have to be used so that relative information on the filler-filler and the filler-polymer networks are obtained.

It is relatively well-established that reinforcing fillers, such as carbon black and (silanated) high structure silica, bring substantial changes in the viscoelastic properties of filled compounds, both in the linear and the nonlinear domains. Nonlinear viscoelastic properties do become important either when materials are submitted to large strain or when a complex morphology develops in the materials owing to self-structuring effects of complex rubber-filler entities, or through a combination of both effects. Large strains clearly concern most of the processing operations but it is also well-known by processing engineers that filled compounds are less prone to large elasticity effects (e.g., reduced extrudate swell, lower severity of melt fracture, etc.) and are paradoxically easier to process than pure, unfilled, elastomers. Linear and nonlinear viscoelastic investigations are thus the methods of choice to document the important properties of filled

Correspondence to: J. L. Leblanc (jean.leblanc@ifoca.com).

TABLE I
Compounds Formulations and Mixing Data

Sample code	SBR00	SBR0N[a]	SBR05	SBR10	SBR15[a]	SBR25	SBR30	SBR33	SBR35	SBR40	SBR50
Ingredient	phr	phr	phr	phr	phr	phr	phr	phr	phr	phr	phr
SBR 1500[b]	100	100	100	100	100	100	100	100	100	100	100
N330	–	–	5	10	15	25	30	33	35	40	50
Naphtenic Oil	5	–	5	5	5	5	5	5	5	5	5
Zinc oxide	5	5	5	5	5	5	5	5	5	5	5
Stearic acid	3	3	3	3	3	3	3	3	3	3	3
TMQ[c]	2	2	2	2	2	2	2	2	2	2	2
IPPD[d]	1	1	1	1	1	1	1	1	1	1	1
Φ_{black}	0.0000	0.0000	0.0220	0.0431	0.0632	0.1011	0.1189	0.1293	0.1360	0.1525	0.1836
Φ_{solids}[e]	0.0075	0.0078	0.0293	0.0502	0.0703	0.1079	0.1255	0.1358	0.1425	0.1589	0.1898
ME, MJ/m^3	423.6	560.1	441.9	526.7	548.1	611	623.6	633	658.2	710	732.5
T_{end} (°C)	110	105	113	116	114	114	116	118	121	121	124

[a] Compounds SBR0N (no oil/blackl) and SBR15 (15 phr Carbon Black) are additional samples, prepared at the end of the test program.
[b] Buna SBR 1500 (Lanxess).
[c] Trimethylquinoline, polymerized.
[d] *N*-Isopropyl-*N*′-phenyl-*p*-phenylene diamine.
[e] solids = Carbon Black + Zinc Oxide. Specific gravity data used to calculate compounding ingredients volume fractions (g/cm^3): SBR1500: 0.93; N330: 1.86; Oil: 0.98; ZnO: 5.57; St.Acid: 0.92; TMQ: 1.08; IPPD: 1.17.

compounds but other information, either with respect to the compounding operations or to the quality of the obtained compounds, are necessary if one want to shed some light on the likely origin of the engineering properties largely used today.

The objectives of this work were to consider a direct method for measuring carbon black agglomeration, and to combine its results with advanced rheological measurements. To minimize variables, an ideal standard SBR1500 formulation without curatives was selected so that various compounds with carbon black contents in the 0−0.184 volume fraction range were prepared in carefully controlled lab-mixing conditions. Reported experimental results are dealing with the microscopic characterization of the dispersion, the linear, and the nonlinear viscoelastic properties. Through the appropriate experimental strategy, the reproducibility and repeatability of the experiments, as well as the storage stability of the materials and the (lack of) strain history effects were concomitantly assessed so that an overall validity can be given to the conclusion of the work.

TEST MATERIALS, DESCRIPTION, AND PREPARATION

A series of carbon black SBR 1500 compounds, as described in Table I, were prepared in a Haake Rheocord 90 laboratory mixer, equipped with a 300 cm^3 chamber and Banbury type rotors. Rotors rate was 40 RPM, fill factor 0.7 and a dead-weight of 5 kg was used to close the chamber. All mixing operations started at 80°C. The procedure was as follows: with the rotors running and the temperature stabilized, the rubber load, cut in small pieces, was first introduced and masticated for 30 s; then half the carbon black content, the zinc oxide and the stearic acid were introduced with the assistance of the ram, then the rest of the compounding ingredients were added and the mixing maintained until 5 minutes were elapsed. The rotors were stopped, the mixer opened, and the collected batch was passed 10 times without banding on a two roll mill so that a sheet was obtained, which was left to cool down on a stainless steel bench. Test compounds were stored in darkness, at room temperature. Note that compounds SBR0N (no oil, no black) and SBR15 (15 phr N330) were prepared two months after the initial test program, as complementary experiments for supporting certain aspects of results analysis.

The highest carbon black loaded batch corresponds approximately to an ASTM standard formulation,[1] with a lower oil level however, and a reinforced protective system to ensure a better temperature and ageing stability. The other batches were designed to be below and above the so-called percolation level ($\approx$ 0.13) in regards to the carbon black. Note that such a critical filler level is an application of a mathematical concept from the percolation theory, which by definition refers to the occurrence of long-range connectivity in random systems. If carbon aggregates are assimilated to spheres roughly arranged in a compact manner such as the face-centered cubic system, then percolation threshold of around 0.120 (site percolation) to around 0.137 (bond percolation) can be calculated.[2,3] Electrical conductivity measurements tend to yield significantly lower values for the percolation

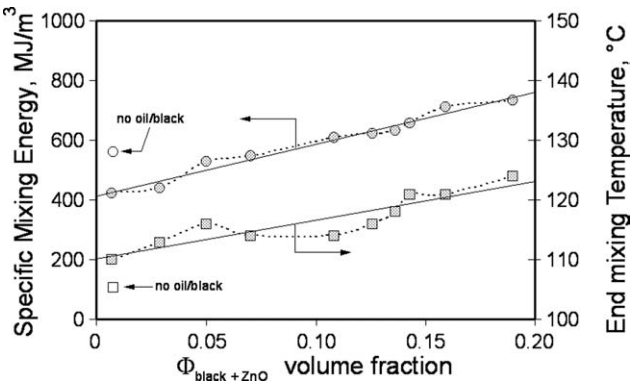

Figure 1 Mixing data versus solid ingredients volume fraction; SBR 1500/N330 compounds; the straight lines correspond to the following equations: $ME(MJ/m^3) = 412.7 + 1735.1 \times \Phi_{solids}; r^2 = 0.98$ and $T_{end}(^{\circ}C) = 110.2 + 64.2 \times \Phi_{solids}; r^2 = 0.81$.

threshold in rubber-carbon black composites[4] but, electrically such systems are extremely heterogeneous and, in the authors' opinion, theoretical rather than (conductivity) experimental threshold values are more relevant in what the mechanical and rheological properties are concerned. One notes that the 30, 33, and 35 phr N330 batches are precisely focused on this critical level. Specific mixing energy data (ME, MJ/m^3) were calculated from the integrations of the recorded torque curves, as provided by the Haake mixer, according to:

$$ME = \frac{\Sigma Tq \times S_{rotors}}{V_{cpd}} \quad (1)$$

where Σ_{Tq} is the overall torque reading (N.m min), S_{rotors} the RPM, and V_{vol} the volume of the batch (m^3). A sample cut from the bale and molded at 100°C for 5 min as a 2 mm thick sheet was also included in the testing program, under the code name SBRGM.

As seen in Table I, there are direct relationships between the carbon black loading and the operational mixing data. The overall mixing time, the fill factor and the ram dead-weight were the same when preparing all compounds, so that both the overall mixing energy and the final mix temperature can somewhat be considered as typical compounding information, essentially controlled by the carbon black dispersion process and hence the developing rubber-filler interactions. Figure 1 shows such data versus the carbon black + zinc oxide volume fraction. Linear relationships can be fitted to such data, with a better correlation coefficient for specific mixing energy than for end mixing temperature. With respect to the lower accuracy in measuring the latter, one would not assign any particular meaning to deviations with respect to the linear trend. A similar graph is produced when using the carbon black volume fraction. Such data do agree well with the obvious fact that the higher the ingredients loading the larger the overall energy consumption at equal mixing time. The higher end mix temperature with higher loading reflects the expected viscosity increase, and hence the larger viscoelastic dissipation, when adding (solid) ingredients to an elastomer. Expectedly the no oil/no black compound requires a significantly higher mixing energy level than the zero black compounds. The softening/plasticizing role of the processing oil is thus clearly seen at this stage.

CHARACTERIZATION OF CARBON BLACK DISPERSION

Principle of the measuring technique

The mixing process as defined by Johnson[5] consists of "incorporation, dispersion, distribution, and plasticization." He further defines dispersion as "the process during which the filler agglomerates are reduced to their ultimate size and dispersed in the rubber." Physical properties and end product performance are a combination of the compound properties as well as the rheological properties.[5,6] It is obvious that polymer and filler types determine many of the product's qualities, but the specific process of filler dispersion has been shown to have effects from product appearance to critical performance properties.[7] These include failure properties such as tensile, tear, abrasion and fatigue resistance, stiffness properties such as hardness and modulus, and dynamic properties such as tan delta.[8–10] According to Boonstra, in the steps of the rubber product manufacturing process, perhaps the one that offers the most variability is the mixing process.[6]

It should be noted that incorporation is the step in the mixing process where wetting occurs. Carbon black does not incorporate at the same rate, or with the same mixing energy in different polymers. For instance it occurs faster in NR than in SBR as used here.

Measurement of incorporation is generally not made directly, but is rather a function of the mixing energy. The critical influence of carbon black dispersion, also referred to as disagglomeration, has made the measurement of dispersion a widely documented topic. Hess gives a good introduction to carbon black dispersion and describes various methods to characterize dispersion.[7] These methods can broadly be put into three categories: (1) electrical methods, (2) mechanical methods, and (3) optical/microscopic methods.[11]

One discerning characteristic of these methods is the measurement range of the test. Gerspacher and

O'Farrell generally describe the methods and the size factor of measurements.[12] The AFM and TEM techniques can measure at the aggregate level (i.e., submicron), but they are time consuming and the equipment is expensive. In addition, such methods may fail to give adequate information regarding "large objects." Optical techniques, on the other hand, typically measure in the range of 10 microns and larger leaving the aggregate level ignored. The visual, optical comparison methods using reflected light usually examine a cut or torn surface that has been shown to relate to the relative degree of dispersion.[7] Based on this observation the mechanical method using a stylus to measure surface roughness was employed to quantify the measurement.[9] This method gives a measure of the height and the frequency of the roughness peaks. Leigh-Dugmore[13] suggested an optical microscope technique utilizing transmitted light where the volume of undispersed carbon black was compared to the total volume of the carbon black in the compound. The equation was modified by Medalia[14] to give a more precise measure of carbon black dispersion. The optical comparison techniques, Leigh-Dugmore and stylus techniques are detailed in ASTM D2663.[15]

Of the methods described above the optical comparison technique proved to be the fastest and to provide suitable information for quality control.[16] Persson significantly improved the optical technique by employing a split screen comparison.[17] This allowed the unknown specimen to be shown directly next to the known standard. The comparisons were further improved by developing mathematical algorithms that automatically calculate the dispersion rating. The basis of these algorithms is to duplicate the human, visual comparison, but to do it more accurately, reproducibly, and without operator's error.

A basic limitation of the use of predetermined reference scales is that different fillers and different polymers exhibit different surface characteristics when mixed. To overcome this, additional reference scales were established for various polymer/filler blends. These scales were based on 10 samples each of five compounds mixed to varying degrees. These specimens were measured at 100× magnification. The general relationship of these scales is described by Andersson et al.[18] Although the filler type and/or polymer are shown for each scale, the concept of the application is visual comparison. A scale is chosen that best suits the observed surface roughness of the compound being tested. The advantage of such a reflected light optical comparison is that the dispersion rating is fast and definitive. The mathematical algorithm further improves the method by removing the judgment of the operator from the result. The resulting dispersion rating is one-dimensional. It is an overview of the surface of the material quantitatively and objectively compared to a standard. This has repeatedly been shown to accurately describe dispersion.[7,10,15,16] The surface of the specimen, however, is not one-dimensional. The surface has hills and valleys of varying occurrences. The quantification of these surface values has generally been done by the mechanical stylus method as described in detail by Vegvari et al.[9] A method of quantifying the surface roughness in two dimensions was described by Andersson et al.[18] in which the reflected light optical method, generally used to determine a comparative dispersion rating, is expanded to give quantitative data as to the size and number of the disturbances. It is important to note here, that the surface roughness does not show the actual filler agglomerates. It is assumed that as the sample is cut, large agglomerates are pushed to one side or the other leaving the contoured surface of the rubber.[17] The diameter and frequency of the surface contours are measured using image processing. These contours are referred to as "nodges" to differentiate them from actual agglomerates. This data is presented in histogram form of count versus nodge diameter.

With the data available from the histogram one can look at specific size nodges and determine additional information regarding the compound's dispersion. Rather than a comparative rating judged against various reference scales, it would be an improvement to have a more definitive measure of the compound's dispersion. To consider this, let's have a look at the method developed by Leigh-Dugmore[13] and specified in ASTM D2663.[15] The basis of the Leigh-Dugmore method is that a specimen is microtomed and examined under a light microscope at 70× to 100× magnification. The number of agglomerates, U, as seen through 10,000 so-called "graticule" squares is compared with the volume percentage of the carbon black, L, in the compound. The percent of dispersed carbon black is:

$$\text{Dispersion, } \% = 100 - \frac{SU}{L} \tag{2}$$

where:

U = Number of graticule squares that are at least half filled with carbon black.

L = Volume percentage of carbon black in the compound.

S = Swelling factor of the specimen based on area (see below).

The microtome technique requires the use of naphtha to remove the specimen from the knife-edge. This results in swelling of the specimen. By measuring the specimen before and after application of the naphtha, an area-swelling factor, S, can be assessed and used in the calculation above.

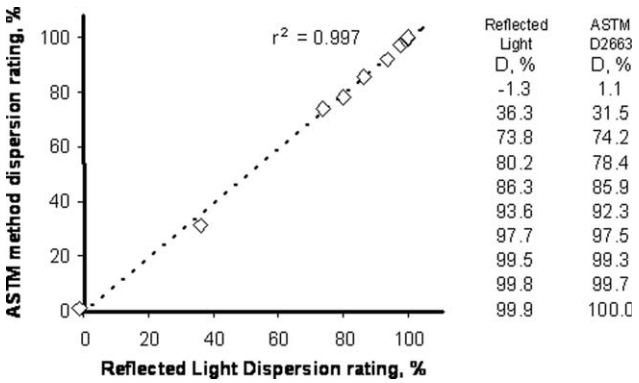

Reflected Light D, %	ASTM D2663 D, %
-1.3	1.1
36.3	31.5
73.8	74.2
80.2	78.4
86.3	85.9
93.6	92.3
97.7	97.5
99.5	99.3
99.8	99.7
99.9	100.0

Figure 2 Comparing dispersion measurements using either the transmitted light (ASTM method) or the reflected light techniques; note that the negative rating value obtained from the reflected light technique is only mathematical artifact and has no physical meaning; either zero or a small positive value could be considered instead.

The ASTM D2663, Method B, standard is explicit in using the 10,000 graticule squares for estimating the area of the carbon black agglomerates. Today, image processing can simplify this tedious task. If *U*% is the percent undispersed agglomerate count of carbon black, 10,000 is the total number of squares in the field, and *U* is the number of squares half filled with agglomerates in the field, then:

$$\mathrm{U\%} = 100\left(\frac{\mathrm{U}}{10,000}\right) = \frac{\mathrm{U}}{100}$$
$$\mathrm{U} = 100\mathrm{U\%}$$

Substituting into eq. (2) yields:

$$\text{Dispersion D\%} = 100 - \mathrm{S}\left(\frac{100\mathrm{U\%}}{\mathrm{L}}\right) = 100\left(1 - \frac{\mathrm{SU\%}}{\mathrm{L}}\right) \quad (3)$$

It is important to note that ASTM D2663 states that the count of *U* encompasses agglomerates down to about 5 μm. It is assumed here that any carbon black agglomerate smaller than this threshold represents fully dispersed carbon black. Image processing then would necessitate that the area calculated for *U*% excludes any contribution from agglomerates less than this threshold.

Medalia[14] commented that the Leigh-Dugmore calculation assumes that the carbon black agglomerate is composed of solid carbon just as are the fully dispersed aggregates. According to him, however, the volume of carbon black in the agglomerate may vary according to several factors including the bulk density of the black, compression of the agglomerates during mixing, and the presence of oils and polymers in the agglomerates. Medalia also noted that since the agglomerates are not 100 % carbon, they might swell with the application of naphtha.[13] He then revised the Leigh-Dugmore calculation for a new dispersion rating, D_n as follows:

$$\text{Dispersion Dn, \%} = 100 - \frac{\nu \mathrm{US}}{\mathrm{AL}} \quad (4)$$

where ν = the average volume fraction of black in the agglomerate and A = the area swelling factor of the agglomerate.

The importance of this lies in the fact that the Leigh-Dugmore calculation may result in negative percent dispersion ratings. If the calculation of Medalia is applied, the actual percent dispersion will always be greater than that calculated by Leigh-Dugmore.

To apply these calculations to the reflected light data, let us consider the histogram data and the method for determining the nodge count. The nodge size and count are determined by optical image analysis of a freshly cut surface.[19] As the specimen is cut the underlying agglomerates are pushed to one side or another resulting in hills and valleys on the cut surface. The resulting hill or valley represents agglomerate or several agglomerates under the surface of the cut. The nodge diameter that is calculated from these surfaces is larger than the underlying agglomerate. This is important, since if one applies either eqs. (2), (3), or (4) above, one must first have some method for disregarding small agglomerates (those less than 5 μm) or disregarding small nodges that are covering the agglomerates.

Given the histogram data, the area represented by the nodges is easily determined from the radius and frequency for all nodges greater than the determined nodge threshold. Then knowing the scan area, the percent nodge area, *U*%, can be determined.

The purpose of the following experiment was to determine if a correlation exists between the ASTM D2663, method B, transmitted light technique, and the reflected light technique described, and to present examples of the new calculation. Figure 2 shows the results of this study, essentially that both methods give the same results.

Carbon black dispersion or disagglomeration could in principle occur by three mechanisms: (1) splitting of the agglomerate due to shear forces, (2) erosion, and (3) collision of agglomerates. The splitting of agglomerates increases with increased viscosity, and with increased elasticity. Astruc[20] performed optical-rheological experiments to observe the effect of elasticity on the erosion process of carbon black agglomerates, in controlled shear viscosity conditions. It was observed that by increasing elasticity at a constant apparent shear stress, erosion is significantly reduced. Therefore it can be assumed that erosion occurs at larger shear stresses in a

TABLE II
Dispersion Results on SBR1500/N330 Black Compounds, as Measured Through Reflected Light Microscopy, and Calculation with eq. (3)

			Dispersion measurement results			
			D (%)	*D* (%)	*D* (%)	*D* (%)
Sample code	CB vol. fraction Φ_{black}	CB + ZnO vol. fract. Φ_{solids}	Threshold > 17	Threshold > 20	Threshold > 23	Threshold > 26
SBR00	0	0.008	97.4	98.3	98.6	98.9
SBR05	0.022	0.029	78.4	78.9	80.3	81.8
SBR10	0.043	0.050	80.9	82.1	82.3	82.7
SBR25	0.101	0.108	86.3	86.4	87.2	87.5
SBR30	0.119	0.126	86.6	86.7	87.3	87.3
SBR33	0.129	0.136	88.2	88.8	89.5	89.7
SBR35	0.136	0.143	89.3	90.2	90.4	91
SBR40	0.153	0.159	91.7	92.1	92.8	92.4
SBR50	0.184	0.190	91.9	92.4	93.1	93.2

viscoelastic matrix, with increasing elasticity, than it would in a Newtonian fluid. The third mechanism of collision is likely occurring when the matrix viscosity is sufficiently low and therefore is playing a nearly insignificant role of quantifiable dispersion in rubber systems.

From the above description it is clear that volume fraction of filler is the key component in understanding the dispersion quality of a mix. It has been noted that with an increased volume of carbon black an increase in viscosity occurs. Since increasing viscosity generally increases the mechanism of filler dispersion of agglomerate, splitting the addition of black should by that common wisdom lead to increased dispersion. It is likely however that it is not the overall change in viscosity of the matrix that causes this effect, but rather a change in local shear stress due to the presence of an elastic solid, the carbon black agglomerate, in the region where splitting occurs.

Dispersion measurement results

Dispersion measurement results are given in Table II, with respect to defined threshold values. The measuring technique not only considers carbon black particles but also any other "solid" particle that might be detected in the compound, for instance zinc oxide particle or solid chemicals that would have not been fused during mixing. Consequently dispersion measurement results are also obtained on the zero black compound. Table II essentially shows that the dispersion rating of the lowest carbon black loaded compound is significantly smaller than the zero black one. This means that a slight amount of carbon black helps dispersing the other compounding ingredients, likely through a better spreading of mixing stresses throughout the material in the mixing chamber. Then the dispersion rating steadily increases with carbon black volume fraction with little, if any, difference when considering various threshold values. Using either the carbon black or the carbon black + zinc oxide volume fractions does not change the observed pattern.

Discussion of dispersion data

The reflected light method for measuring the roughness of a cut surface has been shown to provide a fast and definitive measure of dispersion. Because the surface roughness is dependent on not only dispersion, but also polymers, fillers and filler loadings, several different scales have been developed to enable a variety of compounds to be analyzed.

These scales provide a good relative measure of dispersion. It would also be helpful to know, even on a relative basis, an approximate percent dispersion. By applying a modified Leigh-Dugmore calculation to the histogram data obtained from the reflected light method, a relative percent dispersion was obtained. These results relate well with the values obtained when applying the Leigh-Dugmore calculation and further provide detailed dispersion information in a fast and quantitative measurement. The method provides a more universal scale for measuring dispersion and is equally applicable to vulcanized and unvulcanized specimens since the described experiment did not have a curing agent adding, the unvulcanized measurement was crucial.

More importantly the volume fraction of Carbon Black in the experimental SBR compounds shows that dispersion does in fact improve with loading. It can be assumed that this occurs not only from the increase in viscosity, but also as a result of the physical forces of disagglomeration of tightly agglomerated carbon black, as the shear stress increases in the local areas being observed. There is also an inflection point, which occurs near the hypothetical level predicted by percolation theory. This suggests that once a filler network is established, in addition to the polymer filler network, dispersion improves.

LINEAR VISCOELASTIC ANALYSIS

Experimental approach for linear viscoelasticity

A convenient approach to document the linear viscoelastic properties consists in performing frequency sweep experiments at various temperatures and, with respect to the time-temperature superposition principle, to build mastercurves at a reference temperature. Such experiments were performed in the 60−160°C range with a "Rubber Process Analyzer," RPA 2000®, (Alpha Technologies, now a division of Dynisco LLC, Franklin, MA), by using the built-in capabilities of the instrument. The following test protocol was used: a sample is cut out of an approximately 2.5 mm thick sheet with a circular die of 4 cm diameter and its weight is controlled so that its volume is around 3.1 cm^3. The sample is loaded in the RPA test cavity, previously thermally stabilized at 100°C. As soon as the die is closed, the temperature is decreased to 60°C. After 3 minutes dwell time, a frequency sweep sequence (5 steps), with 1° strain angle is applied, then the temperature is raised by 20°C and after a dwell time of 2 min, the frequency sweep sequence is repeated, then the temperature is raised again, and so on up to 160°C. Such a test lasts around 30 minutes. Two samples per batch are tested with entangled frequency steps so to that by combining the results of both tests 10 applied frequencies in the 0.1 to 17 Hz are probed. Using a VBA macro-instruction program both tests results, as recorded by the built-in system of the RPA, are loaded in an Excel worksheet. A data handling program, written in MathCad®8.0 (MathSoft, now PTC, Needham, MA) is then extracting the shift factors for G', G'', and G^* experimental data, calculating the mastercurves at the selected reference temperature and returning all results to the Excel worksheet. The whole data treatment lasts a few second per sample.

Linear viscoelastic results

Figure 3 shows typical linear viscoelastic results as obtained from frequency-temperature sweep experiments on the 33 phr N330 filled SBR compound. G' and G'' data as measured during test campaign 2 are shown in the top graphs; test campaign 1 data nearly superimposed. The shift factors are given in the bottom left graphs with respect to a reference temperature of 100°C. The curves were drawn using a WLF type equation and the following (fitted) constant: for G', $C_1 = 2.143$ and $C_2 = 116.6$ respectively; for G'', $C_1 = 2.100$ and $C_2 = 114.6$, respectively. Differences are marginal and consequently the curves drawn cannot be distinguished from each other. Mastercurves at 100°C are drawn in the bottom right graphs and because results from test campaigns are superimposed, it can be concluded that the compound was not affected by any ageing effect at room temperature over the 2 months study period. It is worth noting that, with respect to the experimental frequency window (i.e., 0.1–17 Hz), the time-temperature superposition principle allows the dynamic properties of the materials to be obtained over about twice the tested range.

All mastercurves determined for the tested compounds exhibit the same shape, except that the curves are shifted towards higher modulus values as filler content increases. Figure 4 shows the two extremes cases, either the gum rubber or the 50 phr filled compound. In both cases, the G' and the G'' mastercurves clearly show that, at 100°C, the materials are in their terminal (or flow) region but the respective positions of the elastic and the viscous moduli curves demonstrate that the gum elastomer behaves as a solid-like material rather than as a truly viscoelastic fluid. Indeed, over the near four decades of investigated frequency, G' is always higher than G'' and no G'–G'' crossover point can reasonably be foreseen. Adding carbon black changes noting to this behavior, the filled compound is still a solid-like "fluid" but is harder to flow because both the elastic and the viscous moduli are significantly enhanced by the presence of the filler particles. One notes that the G'' curve for the gum rubber clearly shows the occurrence of the rubbery plateau at around 100 Hz. Low filled compounds up to 10–25 phr allow also the beginning of such a plateau to be detected but above 30 phr, the G'' curves exhibit only a continuous increase over the whole frequency range accessible through the time-temperature superposition. Such observations are in sharp contrast with most dynamic data reported for thermoplastic materials, which generally exhibit a crossover of the G' and G'' curves at the beginning of the terminal zone.

A convenient manner to compare the mastercurves and somewhat quantify the differences due to compounding variations consists in reading (through local Lagrangian interpolation) G' and G'' data at well-selected frequencies. Figure 5 shows the values read at 1 Hz, that is, approximately the middle of the experimental frequency range (on log scale) and at 100 Hz, that is, as extrapolated from measured data through the mastercurves. Compounding variations were considered either with respect to the volume fraction of all the ingredients (i.e., black + chemicals) or with respect to the volume fraction of the "solid" ingredients, that is, the black and the zinc oxide. The reasons for such representations are as follows: first it allows the gum rubber to be compared with the compound, second it allows to distinguish the plasticizing effect of the "nonsoluble" ingredients, that is all chemicals except the carbon black and the zinc oxide, third it permits

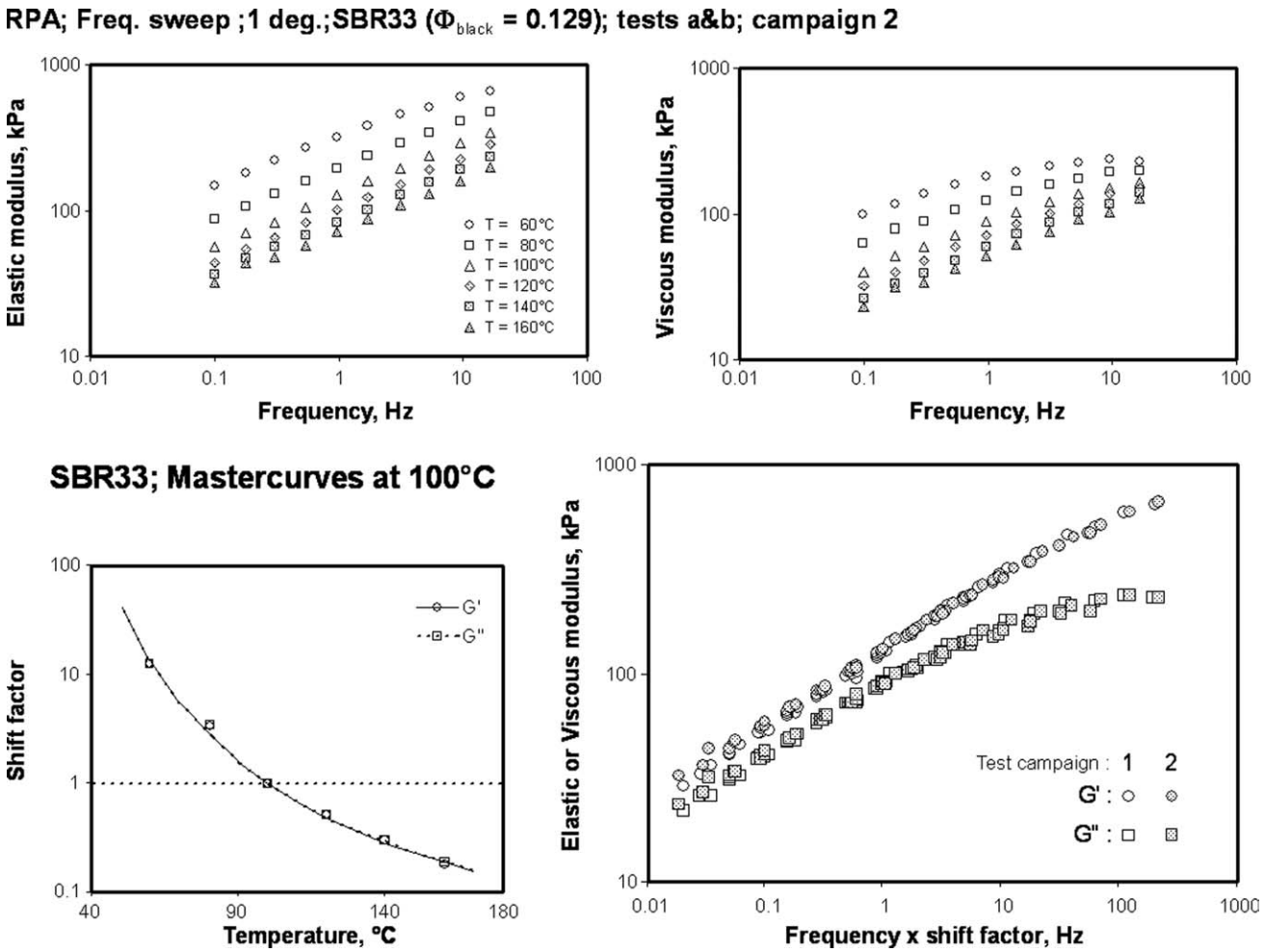

Figure 3 Frequency sweep experiments on the 33 phr N330 filled SBR 1500 compound; G' and G'' measured data and mastercurves at 100°C.

to consider the effect of mixing on the dynamic properties.

Let us consider first the variation of the elastic modulus (left graphs). Clearly the higher the frequency the larger are the effects of the compounding ingredients with, expectedly, the carbon black playing the most significant role. The gum rubber has data points on the vertical axis and the first points

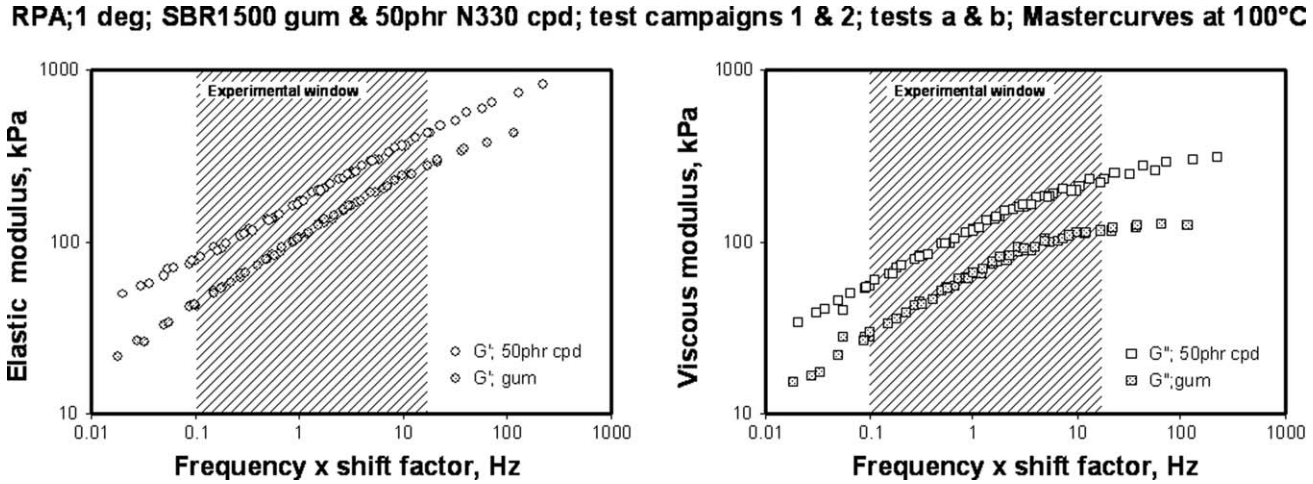

Figure 4 Frequency sweep experiments on gum SBR 1500 and the 50phr N330 filled compound; G' and G'' mastercurves at 100°C.

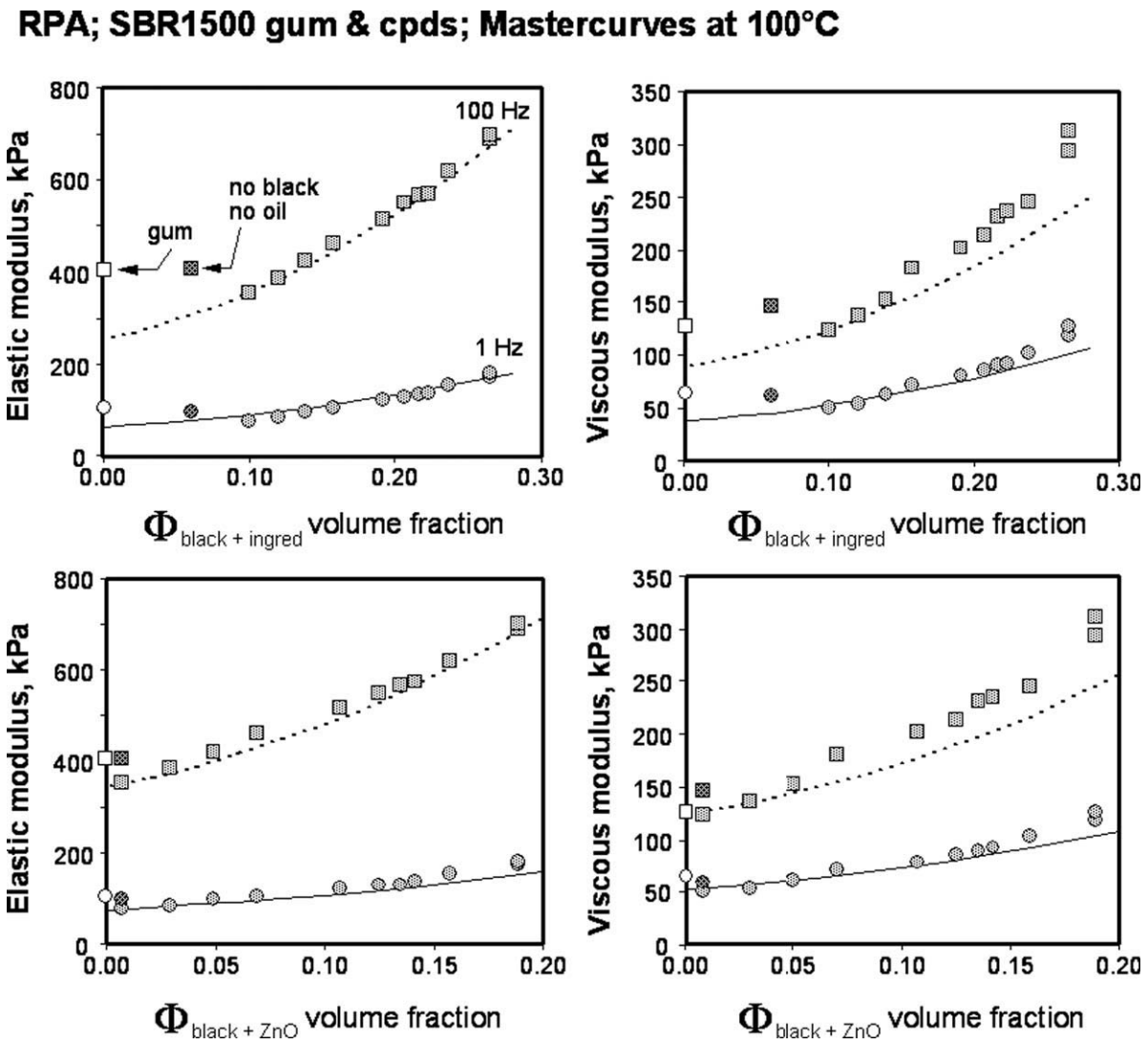

Figure 5 Effect of compounding ingredients on viscoelastic properties of carbon black filled SBR 1500 compounds, at 1 and 100 Hz.

in the graph area correspond to the no oil/black compound. The plasticizing effect of the chemicals is clearly documented when comparing the top and the bottom graphs. Quite significantly the no oil/black compound exhibits the same elastic moduli as the gum sample, thus indicating that, in sharp contrast with the oil's plasticizing effect, the mastication associated with the 5.5 min. mixing process has practically no effect. Such observations correspond well to long reported results by Baranwal and Jacobs[21] who demonstrated that even after extended mixing time (i.e., up to 180 min on open mill), the number molecular weight of SBR1502 type materials is barely changed and only a progressive lowering of MWD is observed. Figure 5 shows also that more than 15 phr of carbon black are necessary to compensate the oil's softening effect. The curves in the graph were drawn with a simple Guth and Gold type equation [i.e., $P_{cpd} = P_{mat}(1 + 2.5\Phi + 14.1\Phi^2)$ where P_{cpd} and P_{mat} are the properties of the compound and the matrix, respectively and Φ the volume fraction considered]. In each case, a simple iterative method was used to select the matrix property value, i.e., the modulus G'_{mat} in the current case, which gives the best fit. As can be seen, this simple model gives a perfect fit for the elastic modulus, up to the highest ingredients load considered, whatever the frequency, but the extrapolated G'_{mat} values are significantly differing from the measured data on the gum rubber. At first sight, this good fit is surprising since the Guth and Gold model was developed with respect to mere hydrodynamic considerations on noninteracting spheres of equal diameter suspended in a simple medium. The key aspect of our observations is however that the modulus value used for the matrix is in fact involving the overall effect of the compounding ingredients, that is, the chemicals and the oil, that plasticize, and the

"solids", that is, the black and the zinc oxide, that reinforce.

The right graphs in Figure 5 show the variation of the viscous modulus with the volume fraction of either all compounding ingredients or the particulate ingredients. The same plasticizing role of the oil is also observed, with however an effect of the test frequency. Again a Guth and Gold type equation was used with G'_{mat} determined by extrapolation. As can be seen the fit is correct only up to a volume fraction of around 0.13−0.14 and the plasticizing effect of the soluble chemicals is clearly detected and fully compensated by the solids ingredients when this critical level is reached. The higher the frequency, the larger are these effects. Such observations suggest that, in what the viscous character of compounds is concerned, the reinforcing effect is likely associated with the occurrence of a network of solid particles, in agreement with dispersion measurements.

NONLINEAR VISCOELASTIC ANALYSIS

Experimental approach for nonlinear viscoelasticity

A fast and convenient technique to investigate the nonlinear viscoelastic response of polymer materials consists in performing strain sweep tests from the lowest up to the highest strain amplitude either permitted by the instrument or before boundary conditions between the sample and the test gap walls ceased to be optimal. Only torsional dynamic rheometers, with a reciprocal cones test chamber whose upper and lower dies are maintained with a sufficient closing force (∼ 15.7 kN), proved to provide very reproducible and meaningful results under large amplitude oscillatory strain (LAOS) conditions. These instruments are essentially rotorless rheometers and are commercially available, for example, the "Rubber Process Analyzer," RPA 2000®, the "Production Process Analyzer," PPA® (Alpha Technologies, now a division of Dynisco LLC, Franklin, MA), the "Moving Die processability tester," MDpt® (TechPro, now a division of Dynisco LLC). All such instruments meet the requirements for standard measurements of rheological properties of unvulcanized rubber,[22] and their measuring principle has been validated through extensive experiments and numerical simulation.[23,24] It is quite clear that, owing to the relatively complicated shape of the test cavity only an average strain situation is achieved but similar comments can be made for most rheometrical techniques. Numerical simulation reveals that the peripheral higher stress region imparted by the closed edge of the cavity has no significant effect on the actually measured dynamic modulus, as experimentally demonstrated.[25]

To extend its capabilities, a RPA 2000®, was purposely modified in our laboratory with the initial objective to develop "Fourier Transform" (FT) rheometry. The modifications brought to the instrument, consist essentially in capturing strain and torque signals, using a 16 bits electronic analogic-digital conversion card. Essentially, Fourier Transform rheometry consists of resolving captured strain and torque signals into their harmonic components by means of the appropriate calculation algorithms. In other terms, the information, gathered in the time domain, is resolved into a representation of the measured material property in the frequency domain, in the form of a spectrum of harmonic components. If the response of the material is strictly linear, then proportionality between (applied) strain and (measured) torque is kept and the torque signal is a simple sinusoid. In such a case the torque spectrum consists only of a single peak at the test frequency. A nonlinear response is characterized by a number of additional peaks at odd multiples of the applied strain frequency. The capabilities of FT rheometry in delivering data likely related with macromolecular characteristics have so far been demonstrated with a number of polymer materials.[26–28]

Test protocols for no-linear viscoelastic investigations consist in performing strain sweep experiments (at fixed frequency and temperature) through two subsequent runs separated by a resting period of 2 min (note: 2 min is an arbitrary choice, but generally found largely sufficient for viscoelastic recovery with most polymer systems tested so far when no permanent structural damage has occurred during the first run). At least two samples of the same material are tested (more if results revealed test material heterogeneity), in such a manner that, through inversion of the strain sequences (i.e., run 1 and run 2), sample fatigue effects are detected, if any. Differences are indeed expected between runs 1 and 2 for materials exhibiting strain memory effects, either permanent or at least not fully dampened after the 2 min resting period. Strain memory effects are practically never observed with gum elastomers and standard carbon black filled compounds but are quite common with certain complex polymer systems, namely highly loaded systems and compounds with short fibers. In any fixed strain and frequency conditions, data acquisition is made to record 10,240 points at the rate of 512 pt/s, that is, 20 cycles at 1.0 Hz or 10 cycles at 0.5 Hz. FT spectra are obtained through calculation on the last 8192 points of the recorded signals. With the RPA, the maximum applicable strain angle depends on the frequency, for instance around 68° (≈ 950 %) at 0.5 Hz, considerably larger than with open cavity cone-plate or parallel disks torsional rheometers. Whatever the frequency however, the lower strain angle limit is practically 0.5° (6.98 %) below which the noise content of the strain signal becomes so high that

measured torque is excessively scattered and likely meaningless.

At low strain amplitude, the RPA suffers a certain harmonic content of the strain signal. An easy correction method was developed for torque harmonics, based on observations made when testing an ideal elastic body, for instance the calibration spring. Essentially, $T(n\omega/\omega)$ data are corrected according to:

$$T(n\omega/1\omega)_{corr} = T(n\omega/1\omega)_{TF} - CF_n \times S(n\omega/1\omega)_{TF} \quad (5)$$

where $T(n\omega/1\omega)_{TF}$ and $S(n\omega/1\omega)_{TF}$ are the nth relative harmonic components of the torque and strain signals respectively, and CF_n the correction factor, as derived from a plot of $T(n\omega/1\omega)$ versus $S(n\omega/1\omega)$, which passes through a minimum and appears to be bounded by a straight line whose slope provides the correction factor. Note that $T(n\omega/1\omega)$ and $S(n\omega/1\omega)$ are relative harmonics (with respect the main harmonic component at the applied frequency) and therefore have no unit; for convenience however such data are expressed in %. The correction method is based on the simple argument that, if the applied strain were perfectly sinusoidal, all $T(n\omega/1\omega)_{TF}$ data points would fall on the vertical axis. Experimentally demonstrated for the third and the fifth relative torque harmonics and also for the so-called "total torque harmonic content", TTHC, that is, the sum $\sum T(n\omega/1\omega)$ of all the odd harmonics up to the 15th, this correction method has the immediate result that at low strain, when the viscoelastic response of the material is expected to be linear, the corrected relative torque harmonics vanish, in agreement with theory.[29]

According to strain sweep test protocols described above, RPA-FT experiments and data treatment yield essentially two types of information, which reflects how the main torque component, that is, $T(1\omega)$, and the relative torque harmonics, that is, $T(n\omega/1\omega)$ and $\sum T(n\omega/1\omega)$ vary with strain amplitude. Such variations are conveniently modeled with simple mathematical relationships.

(RPA-FT) Complex modulus versus Strain amplitude

Whatever the sample tested, no significant differences were seen on complex modulus data, either between tests a and b, or runs 1 and 2, or even between tests results from both test campaigns at constant frequency, either 0.5 or 1.0 Hz. This means that (1) all samples were of excellent quality, that is, similar results from tests a and b, (2) no strain history effects could be detected, that is, no differences between runs 1 and 2, and (3) within a two months period, storage at room temperature did not bring any ageing effects. Consequently, all G^* results were merged in two sets, respective to the two test campaigns. Typical complex modulus G^* versus strain results at 0.5 Hz are shown in Figure 6 for selected samples. Similar results were obtained at 1.0 Hz but expectedly shifted towards slightly higher values. As can be seen, in all cases, results from the two test campaigns cannot be distinguished, within a normal experimental scatter of around 1% at all strains for the gum and the low loaded compounds and 4 to 1% (low strain to high strain) for the highly loaded compounds. It is worth underlining here that G^* data shown in the Figure are derived from the main component of the torque signal, as obtained through FT analysis. Qualitatively similar graphs are obtained when using G^* values from the standard RPA (built in capabilities) but with an error by excess and a slightly larger scatter, particularly in the nonlinear region.

Visible with the gum sample and the zero black compound (top graphs in the Figure), the linear region (i.e., G^* plateau) is clearly observed within the experimental window of the RPA, that is, 6.98–949.46 % strain at 0.5 Hz. Above 25 phr carbon black loading, this is barely the case (bottom left graph) and higher loaded compounds do exhibit a full nonlinear behavior. For a material exhibiting linear viscoelasticity within the experimental window, a plot of G^* versus γ shows the most familiar picture of a plateau region at low strain, then a typical strain dependence, that is well captured through the following equation:

$$G^*(\gamma) = G_f^* + \left[\frac{G_0^* - G_f^*}{1 + (A\gamma)^B}\right] = G_f^* + \left[\frac{G_0^* - G_f^*}{1 + \left(\frac{\gamma}{\gamma_{md}}\right)^B}\right] \quad (6)$$

where G_0^* is the modulus in the linear region, G_f^* the final modulus, $A = 1/\gamma_{md}$ the reverse of the strain for the mid-modulus value, that is, $(G_0^* + G_f^*)/2$, to be reached, and B a parameter related to the strain sensitivity of the material. Curves in Figure 6 were drawn using this model that, indeed, perfectly fit experimental data. Treating experimental results with eq. (6) is thus a very convenient manner not only to pertinently summarize a large number of measured data through a reduced set of significant parameters but also to extract various typical features of materials behavior through easy mathematical handling. For instance the linear-to-nonlinear transition can be unambiguously characterized through a critical strain γ_c that corresponds to the intersection of an horizontal line equal to G_0^* and the line passing through point $(\gamma_{md}, (G_0^* + G_f^*)/2)$ and having a slope equal to the first derivative of eq. (6), calculated at $\gamma_{md} = 1/A$. Figure 6 shows indeed that γ_c decrease with increasing filler loading. Recalculating the

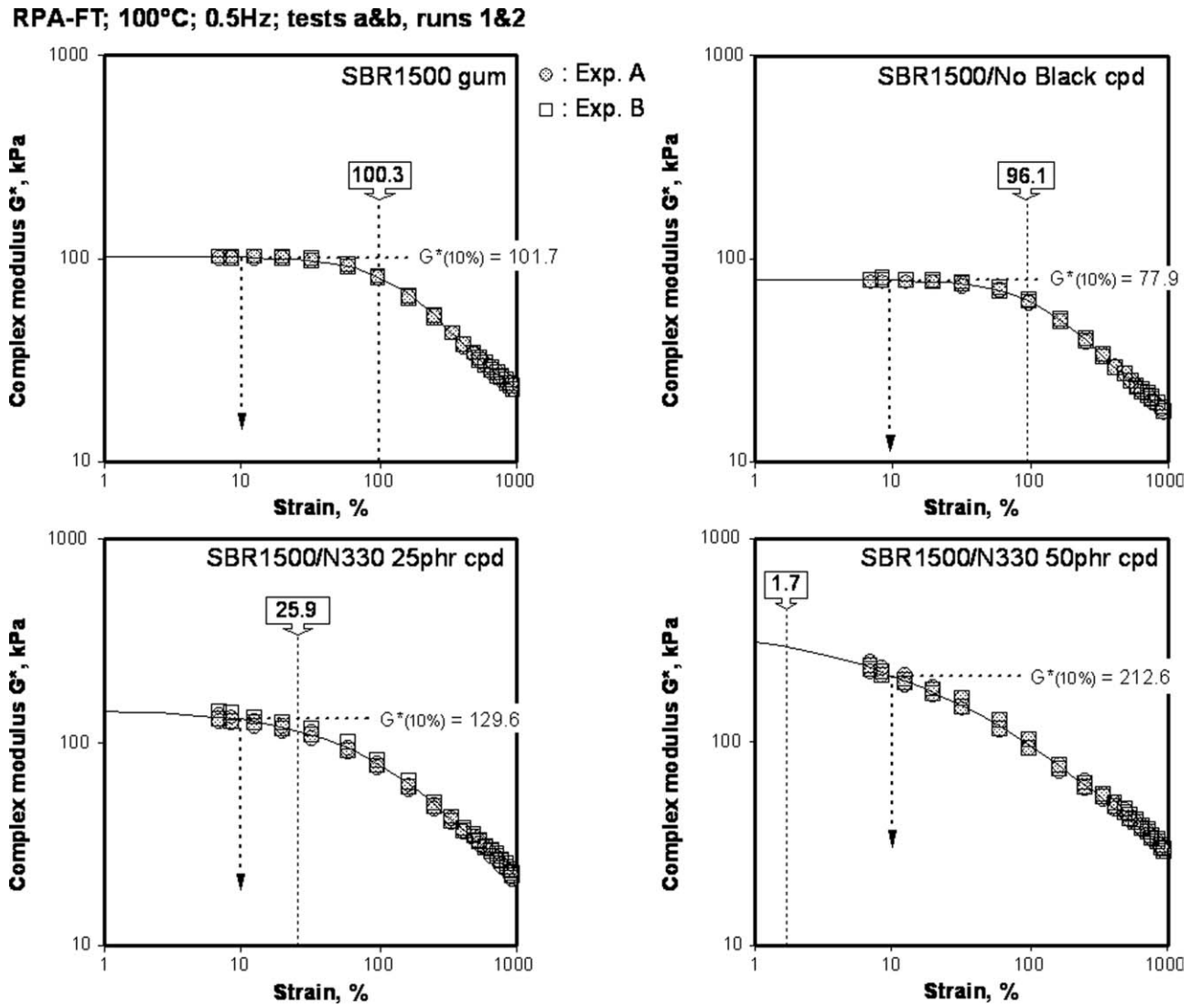

Figure 6 RPA-FT at 0.5 Hz, 100°C; typical complex modulus versus strain variations. Results from two test campaigns are shown, as well as model curves drawn using eq. (6) and typical (calculated) features such the critical strain for linear-to-nonlinear transition and the modulus at 10% strain.

modulus within the experimental window, let's say 10% strain, allows comparing test samples through their true experimental response with a de facto compensation for experimental scatter. Table III gives the parameters of eq. (6) that corresponds to the experimental results gathered with all the tested samples, as well as several (calculated) typical features.

Modeling the variation with strain amplitude of the complex modulus yields a number of parameters that precisely document the effect of compounding ingredients, namely carbon black. In term of modulus, eq. (6) gives either the so-called "linear" complex modulus G_0^*, readily an extrapolation to zero strain of the measured data, or any recalculated $G^*(\gamma)$ value within the experimental window, for example, $G^*(10\%)$. When the tested material exhibits a linear viscoelastic behavior within the RPA experimental window, G_0^* appears less an extrapolated value than a truly measured material property. When the material shows a nonlinear behavior in the experimental windows, then caution must be taken in discussing G_0^* results. A few negative values for G_f^* are reported in Table III. They have obviously no physical meaning and are mere artifacts of the nonlinear fitting algorithm. In fact G_f^* are readily values at infinite strain and are therefore purely hypothetical. Whilst necessary for the goodness of the fit, such data are not considered as relevant in terms of material properties.

Figure 7 shows the complex modulus vs. strain curves for all the tested samples, as drawn using eq. (6) and parameters given in Table III. The strong nonlinear character imparted by the filler above 25

TABLE III
RPA-FT at 100°C, 0.5 Hz Tests on SBR1500 gum and Carbon Black Filled Compounds

Sample	SBR1500 gum	SBR1500 cpd	SBR1500 cpd	SBR1500 cpd	SBR1500 cpd	SBR1500 cpd	SBR1500 cpd	SBR1500 cpd	SBR1500 cpd	SBR1500 cpd	SBR1500 cpd
N330 loading	gum	no black	no oil/bl	5 phr	10 phr	15 phr	25 phr	30 phr	33 phr	35 phr	40 phr	50 phr
Sample code	SBRGM	SBR00	SBR0N	SBR05	SBR10	SBR15	SBR25	SBR30	SBR33	SBR35	SBR40	SBR50
Φ_{rubber}	1.0000	0.8999	0.9400	0.8801	0.8611	0.8430	0.8089	0.7928	0.7835	0.7774	0.7626	0.7346
Φ_{black}	0.0000	0.0000	0.0000	0.0220	0.0431	0.0632	0.1011	0.1189	0.1293	0.1360	0.1525	0.1836
$\Phi_{chemicals}$	0.0000	0.1001	0.0600	0.0979	0.0958	0.0938	0.0900	0.0882	0.0872	0.0865	0.0849	0.0818
G^* vs. Strain model parameters												
G_0^* (kPa)	102.5	78.7	90.9	88.5	99.2	114.1	143.7	163.3	173.5	194.3	234.9	363.7
G_f^*, (kPa)	16.8	12.3	15.1	11.4	10.7	9.7	5.9	3.7	2.6	1.9	−1.5	−3.9
A	0.0050	0.0050	0.0053	0.0055	0.0061	0.0073	0.0092	0.0111	0.0124	0.0149	0.0208	0.0541
$\gamma_{md} = 1/A$ (%)	200	200.0	188.7	181.8	163.9	137.0	108.7	90.1	80.6	67.1	48.1	18.5
B	1.569	1.495	1.482	1.333	1.218	1.067	0.911	0.83	0.795	0.753	0.676	0.586
$r^2 =$	0.9999	0.9999	0.9999	0.9999	0.9999	0.9998	0.9999	0.9999	0.9999	0.9999	0.9999	0.9998
G^* vs. Strain: typical features												
$G_{(10\%)}{}^*$, (kPa)	101.73	77.95	89.94	86.92	96.36	108.07	129.62	141.13	146.19	157.25	174.14	212.63
Slope at $1/A$	−0.168	−0.124	−0.149	−0.141	−0.164	−0.203	−0.289	−0.368	−0.421	−0.540	−0.831	−2.913
Crit.Strain γ_c (%)	100.31	96.09	91.11	77.08	62.15	43.54	25.92	17.90	14.64	10.93	6.07	1.67

Fit parameters of eq. (6) and typical calculated features. Volume fractions for the filler, the rubber, and the other ingredients are also given.

phr (i.e., Φ_{black} above 0.10) is clearly observed. With respect to the results obtained on the gum rubber, one notes that compounding brings a kind of softening effect so that, at low filler content, the compounds exhibit lower modulus data than the gum sample. The inset underlines this effect by considering the (calculated) value of the modulus at 10% strain and documents the strong reinforcing effect of the carbon black so that the modulus is nearly doubled when the filler volume fraction is above the so-called percolation level, that is, ≈ 0.13. However no drastic modulus variation is seen in the region of the percolation level, only a smooth increase.

As expected, both G_0^* and $G^*(10\%)$ increase with carbon black volume fraction and alternatively decrease with the rubber volume fraction. Note that bearing in mind the latter allows considering the effects of all compounding ingredients on the viscoelastic properties of the compound, since the gum rubber can be distinguished from the zero-black compound. Even at the lowest filler level investigated, the modulus increase due to carbon black is largely above the prediction of the well-known Guth and Gold model. This is not surprising since the Guth and Gold model was developed with respect to hydrodynamic considerations only, without paying attention to specific interactions that might develop between the polymer and the filler particles. Modifying the Guth and Gold model with a filler anisotropy factor to multiply the volume fraction or using an effective filler volume fraction as suggested by Medalia[30] does not bring any improvement because the modulus variation with CB volume fraction does not obviously follow a quadratic pattern. It is therefore attractive to consider more (mathematically) suitable models, providing however some physical meaning can be assigned to the additional terms.

Notwithstanding considerations that can be developed about the likely interactions between a polymer matrix and dispersed particles, it is quite obvious that as the filler volume fraction increases the role played by the polymer matrix is bound to decrease until eventually a network of deeply connected particles accounts for most of the observed properties. In other words, as the filler fraction increases, one may expect any mechanical or rheological property to exhibit an asymptotic behavior to a limit that will somewhat involve the so-called maximum packing fraction Φ_m of particles. For particles with simple geometries, e.g., spheres of constant diameter, maximum packing can readily be calculated with respect to given particle arrangements. One would have for instance $\Phi_m = \frac{\pi}{3\sqrt{2}} \approx 0.7405$ for a close hexagonal packing (also called face-centered cubic) of uniform spheres. Primary particles of carbon black are only

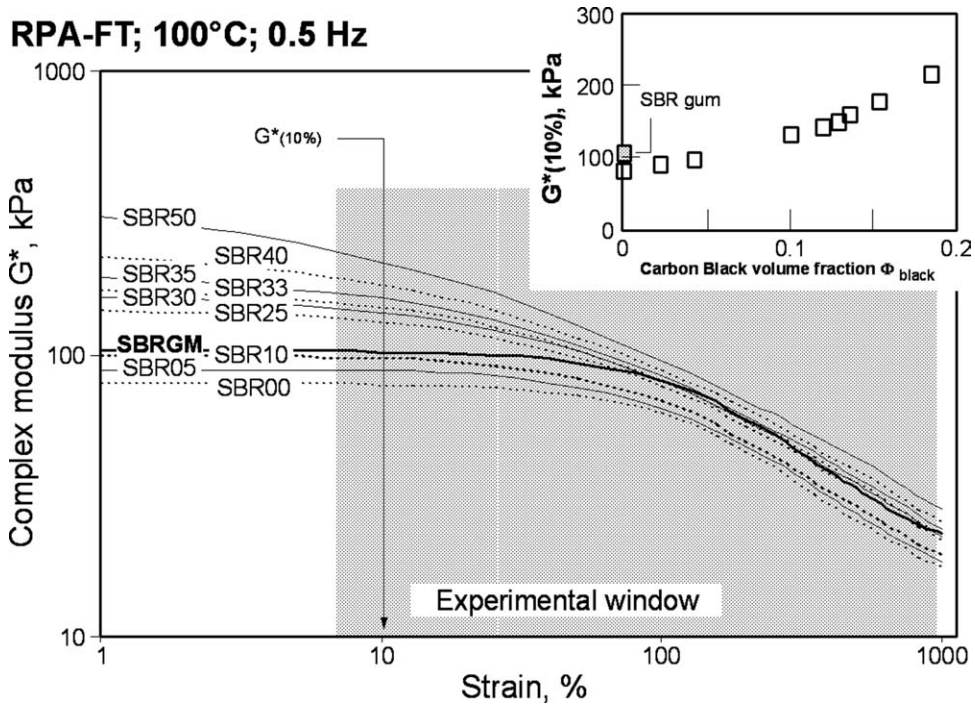

Figure 7 RPA-FT at 100°C, 0.5 Hz on SBR1500 gum and carbon black filled compounds; Complex modulus versus Strain curves are drawn using parameters given in Table III; the inset shows the calculated modulus at 10% strain versus carbon black volume fraction.

considered as a theoretical basis for carbon black grading. These primary particles may be spheres, but in all practical applications the particles can not be reduced to the primary particles, but rather so that the likely maximum packing fraction of aggregates can surely never exceed what could be calculated for a loose cubic packing of uniform spheres, that is, $\Phi_m = \frac{\pi}{6} \approx 0.5236$. Any realistic Φ_m value for reinforcing CB grades is even likely to be significantly smaller than 0.5.

One can consequently consider that, in addition to mere hydrodynamic interactions between filler particles, as readily considered by the Guth and Gold model, other interactions either between particles or between the matrix and the particles account for additional terms. This can physically be explained as a combination of Van de Waals and electrostatic interactions. One manner to mathematically express such views consists in considering a series of terms involving only the filler volume fraction Φ, the maximum packing fraction Φ_m and interaction parameters P_1 and P, as follows:

$$G^*_{cpd}(\Phi) = G^*_{mat}\left[1 + P_1\Phi + P\frac{(P\Phi_m + 1)}{2!\Phi_m}\Phi^2 + P\frac{(P\Phi_m + 1)(P\Phi_m + 2)}{3!\Phi_m^2}\Phi^3 + \ldots\right] \quad (7a)$$

or, in an abridged form:

$$G^*_{cpd}(\Phi) = G^*_{mat}\left[1 + P_1\Phi + \sum_{a=2}^{n} P\frac{\prod_{i=1}^{a-1}(P\Phi_m + 1)}{a!\Phi_m^{a-1}}\Phi^a\right] \quad (7b)$$

Because at very low filler loading, the equation must asymptotically comply with the well-known equation proposed by Einstein, that is, $G^*_{cpd} = G^*_{mat}(1 + 2.5\Phi)$, one would take $P_1 = 2.5$, so that only the number n of additional terms has to be sought for a best fit of experimental data with respect to appropriate values for Φ_m and P.

As illustrated in Figure 8 the model easily meets experimental data with a very small number of parameters. The best fit is obtained with a maximum packing fraction of 0.35 and 15 additional terms. One notes that the parameter P must receive a larger value for the linear modulus G^*_0 than the modulus at 10% strain. It follows that any modulus than could be calculated below 10% strain would be fitted with eq. (7) by changing only the value of P, between 4 and 6. In the high strain region (i.e., $\gamma > 100\%$), where increasing filler content produces a mere upward shifting of the modulus, data are well fitted when using $P = 1$.

Apart from modulus increase, larger carbon black loadings bring a number of modifications in the

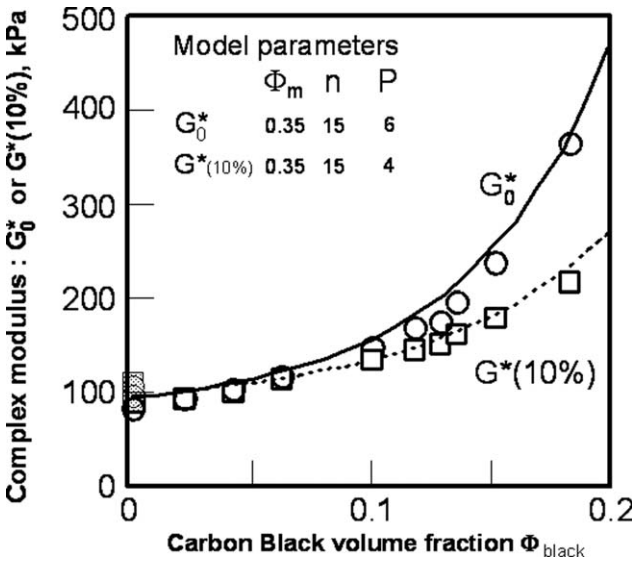

Figure 8 Variation of complex modulus with filler volume fraction in SBR 1500/N330 compounds, as modeled using eq. (7).

viscoelastic character of compounds that will affect the processing behavior. As seen in Table III, both $1/A$ and parameter B decrease with increasing filler content. Parameter B in eq. (6) obviously reflects the strain sensitivity of materials because, all other parameters constant, the larger B, the stepper the G^* versus strain curve. As shown in Figure 9, B varies quasi-linearly with increasing carbon black fraction. If the data are plotted versus the overall compounding ingredient fraction, that is, $\Phi_{\text{black + ingred}}$, the curve is essentially shifted to the right and, with respect to the B parameter measured on the gum rubber, reveals a slight softening effect associated with the nonblack ingredients, essentially the oil, the stearic acid, and the protective chemicals. It is worth noting that the no oil/black compound exhibits the strain sensitivity parameter in the same manner as the no black compound. This means that it is essentially the carbon black that does change the strain sensitivity of compounds. The critical strain γ_c for the linear-to-nonlinear transition provides however more interesting information as it clearly documents how the compounding ingredients (essentially the carbon black in this instance) significantly reduces the linear viscoelastic region. At the level used, the oil appears to have a relatively minor effect on the extent of the linear viscoelastic region.

Such observations suggest a treatment of experimental data so that the effects of compounding ingredients on the viscoelastic behavior are highlighted. Essentially it consists in considering a reduced modulus versus a reduced strain, with respect to a compound measured as a reference. The most obvious choice for the reference compound is the zero black one, by using the overall compounding ingredients fraction, that is, $\Phi_{\text{black + ingred}}$, as relevant formulation parameter. For each tested compound, reduced strain values γ_{red} are calculated from the applied strains γ as follows:

$$\gamma_{\text{red}} = \frac{\gamma \times \gamma_c(\Phi_{b+i})}{\gamma_c(\Phi_{\text{ref}})} \tag{8}$$

where $\gamma_c(\Phi_{b+i})$ and $\gamma_c(\Phi_{\text{ref}})$ are, respectively, the critical strain for the tested and the reference compounds as given in Table III. Similarly reduced modulus values G^*_{red} are calculated from the measured complex modulus G^* as follows:

$$G^*_{\text{red}} = \frac{G^* \times G^*_0(\Phi_{b+i})}{G^*_0(\Phi_{\text{ref}})} \tag{9}$$

where $G^*_0(\Phi_{b+i})$ and $G^*_0(\Phi_{\text{ref}})$ are, respectively, the linear modulus for the tested and the reference compounds as given in Table III. Figure 10 shows the plot of relative complex modulus versus relative strain obtained.

Figure 10 allows for clear understanding how the formulation ingredients, namely carbon black, do affect the viscoelastic properties of compounds. Indeed, all reduced data appear comprised in an envelop area as defined by the complex modulus curve of the reference compound (i.e., the zero black sample) and the curve corresponding to the highest loaded compound, that is readily calculated using eq. (6) but with parameters modified as follows:

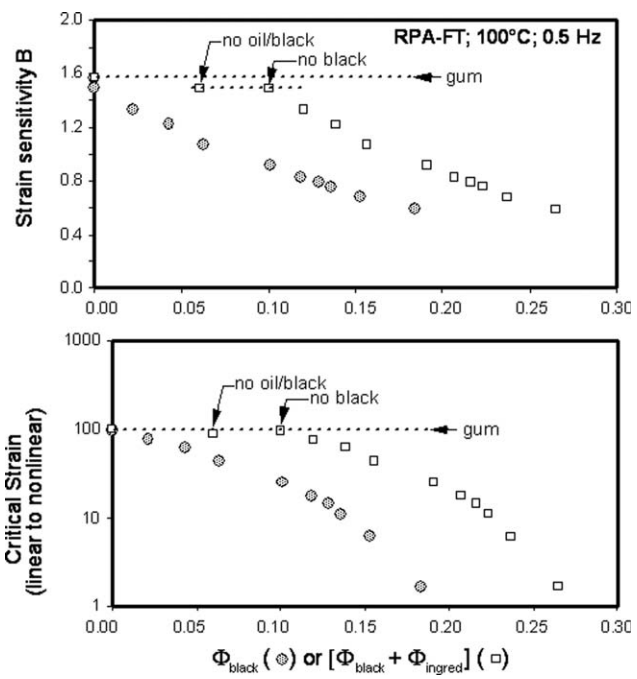

Figure 9 RPA-FT at 100°C, 0.5 Hz on SBR/N330 compounds; effect of compounding ingredients on strain sensitivity (parameter B) and on linear-to-nonlinear transition.

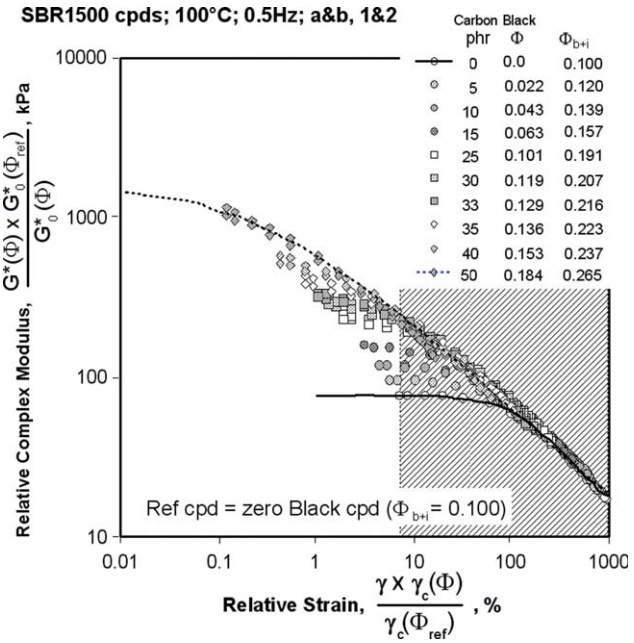

Figure 10 Reduced complex modulus vs. reduced strain for SBR compounds; the dashed area displays the experimental window. [Color figure can be viewed in the online issue, which is available at wileyonlinelibrary.com]

$$G^*_{0,\mathrm{red}} = \frac{G^{*2}_0(\Phi_{\mathrm{b+i}})}{G^*_0(\Phi_{\mathrm{ref}})} \qquad G^*_{\mathrm{f,red}} = \frac{G^{*2}_{\mathrm{f}}(\Phi_{\mathrm{b+i}})}{G^*_{\mathrm{f}}(\Phi_{\mathrm{ref}})}$$
$$A_{\mathrm{red}} = \frac{A(\Phi_{\mathrm{b+i}}) \times \gamma_{\mathrm{c}}(\Phi_{\mathrm{ref}})}{\gamma_{\mathrm{c}}(\Phi_{\mathrm{b+i}})} \qquad B_{\mathrm{red}} = \mathrm{B}(\Phi_{\mathrm{b+i}})\frac{100 - A_{\mathrm{red}}}{100} \tag{10}$$

In the low-strain region, compounding ingredients play a major role, namely with the carbon black that strongly reinforces the (linear) modulus, but also reduces the extent of the linear viscoelastic region so that, highly loaded compounds do not exhibit any linear behavior within the experimental windows. It is essentially the polymer matrix that accounts for the viscoelastic properties of compounds since all powdered ingredients, that is, the carbon black and the zinc oxide, are essentially rigid bodies and cannot therefore dissipate a part of the strain. The viscoelastic matrix and the soft compounding ingredients essentially support an amplified strain, in agreement with long established views.[31] Reducing both the complex modulus and the strain through eq. (10) clearly move the measured data on filled compounds outside of the experimental windows and appears as a more straightforward approach than using a strain amplification factor, depending on the sole filler fraction (through for instance the Guth and Gold formalism). In the high strain region, all reduced data expectedly meets the same curve, which means that most of the ingredients effects on the viscoelastic modulus have (temporarily) vanished. Processing operations necessarily involve large strain, so that the dynamic stress softening (DSS) effect demonstrated in Figure 10 is the key for lower viscosity and hence easier processing at acceptable energy expenses. But DSS is a reversible effect, as clearly demonstrated by the reported experimental results. Indeed, data displayed in Figure 10 are averaged results from runs 1 and 2, since no differences were seen. The DSS effect experienced by compounds during run 1 is totally reproduced during run 2, demonstrating thus reversibility. It must be noted however that, would the rubber matrix exhibit certain special properties such as strain crystallization (i.e., the case of Natural Rubber) or would particular interactions occur between the rubber and the filler particles (e.g., polar interactions), dynamic stress softening could have an irreversible character, at least partially.

(RPA-FT) Torque harmonics vs. Strain amplitude

Odd torque harmonics become significant as strain increases and are therefore considered as the nonlinear viscoelastic "signature" of tested materials. The essential information is obtained by considering the third relative torque harmonic and the so-called "total torque harmonic content," TTHC, that is, the sum $\sum \mathrm{T}(n\omega/1\omega)$ of all the odd harmonics up to the 15th. Figure 11 shows typical variations of torque harmonics with increasing strain amplitude for either the gum SBR 1500 or the 50 phr N330 filled compound, at 0.5 and 1.0 Hz frequency. Within the expected experimental scatter (from 4–5% in the medium strain range where 0.5 and 1.0 Hz data superimpose, down to ≈1% in the high strain region) results are reproducible with no difference between tests a and b, runs 1 and 2 and test campaigns 1 and 2, which further demonstrate the excellent quality and stability of test samples and the lack of sensitivity to strain history. The lack of frequency dependence of relative torque harmonics might be surprising at first sight but has already been observed with various systems, either unfilled[32] or filled elastomers,[33] and polyethylenes[26]; other authors however reported a frequency dependence for model polystyrenes,[34] but somewhat erratic and in a smaller strain range than in our experiments with the modified RPA. It must be noted, however that a frequency span of 0.5 Hz might also be too small to clearly detect frequency effects.

Numerous experiments on various systems have shown that relative torque harmonics vary with strain amplitude in such a manner that an initial S-shape curve appears bounded by a simple linear variation at high strain. Accordingly, the following model was successfully developed to fit results obtained on polymer materials:

$$\mathrm{TH}(\gamma) = (\mathrm{TH_m} + \alpha\gamma_0) \times [1 - \exp(-\mathrm{C}\gamma_0)]^{\mathrm{D}} \tag{11}$$

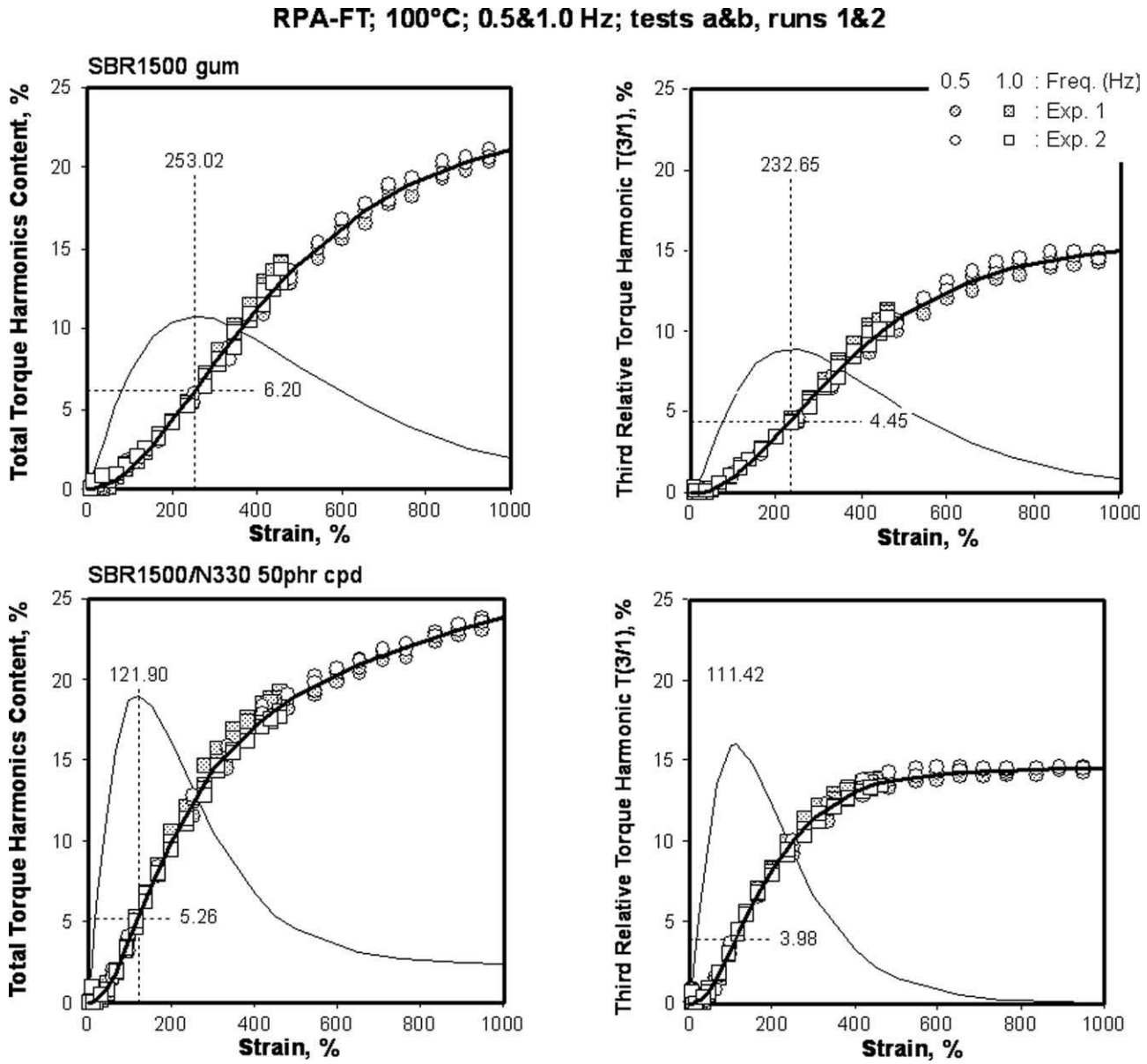

Figure 11 Torque harmonics variation versus strain amplitude at 0.5 and 1.0 Hz for gum SBR 1500 and 50 phr N330 filled compounds; all results from tests a and b, runs 1 and 2; test campaigns 1 and 2 are displayed, as well as the curves fitted with eq. (11) and the first derivatives; the coordinates of the maximum strain sensitivity of torque harmonics are indicated. Note that the first derivative has been multiplied by 300.

where γ_0 is the strain magnitude, TH_m, α, C, and D parameters of the model. TH stands either for a single odd harmonic, that is, $T(3/1)$, $T(5/1)$, ... or the overall harmonic content $\sum T(n\omega/1\omega)$. The member $(TH_m + \alpha\gamma_0)$ expresses an asymptotic linear variation of harmonics in the high strain region, whereas the member $[1 - \exp(-C\gamma_0)]^D$ describes the onset and the development of the nonlinear viscoelastic response, obviously occurring in the low and middle strain region.

The physical meaning of parameters TH_m and α is obvious; parameter D somewhat reflects the extent of the linear viscoelastic region (i.e., where no harmonics are detected), whereas parameter C indicates the strain sensitivity of the nonlinear character. As the strain γ is smaller and smaller, that is, in the linear viscoelastic region, eq. (11) corresponds to asymptotically zero harmonics, in complete agreement with theory. It is worth noting that in using this equation, one may express the strain γ either in degree angle or in %. Obviously all parameters remain the same except C, whose value depends on the unit for γ. The following equality applies for the conversion: $C(\gamma, \text{deg}) = \frac{180\alpha}{100\pi} \times C(\gamma, \%)$, where $\alpha = 0.125$ rad.

Lines correspond to fit obtained with eq. (11) and, as expected, the overall torque harmonic content (TTHC) curve envelops the relative third torque

TABLE IV
RPA-FT at 100°C; 0.5 Hz on SBR Samples; Modeling Relative Harmonics versus Strain with eq. (11)

Sample	SBR1500 Gum	SBR1500 cpd	SBR1500 cpd	SBR1500 cpd	SBR1500 cpd	SBR1500 cpd	SBR1500 cpd	SBR1500 cpd	SBR1500 cpd	SBR1500 cpd	SBR1500 cpd
N330 loading	gum	no black	no oil/bl	5 phr	10 phr	15 phr	25 phr	30 phr	33 phr	35 phr	40 phr	50 phr
Sample code	SBRGM	SBR00	SBR0N	SBR05	SBR10	SBR15	SBR25	SBR30	SBR33	SBR35	SBR40	SBR50
Φ_{rubber}	1.000	0.8999	0.9400	0.8801	0.8611	0.8430	0.8089	0.7928	0.7835	0.7774	0.7626	0.7346
Φ_{black}	0.0000	0.0000	0.0000	0.0220	0.0431	0.0632	0.1011	0.1189	0.1293	0.1360	0.1525	0.1836
$\Phi_{black + ingred}$	0.0000	0.1001	0.0600	0.1199	0.1389	0.1570	0.1911	0.2072	0.2165	0.2226	0.2374	0.2654
Modeling TTHC vs. Strain												
$TTHC_0$ =	23.17	20.88	19.12	19.92	20.21	16.39	20.36	17.19	16.41	17.65	16.72	16.13
α	1.34×10^{-11}	1.62×10^{-11}	0.0019	0.0011	0.0011	0.0056	0.0019	0.0054	0.0062	0.0053	0.0066	0.0079
C	0.0032	0.0037	0.0045	0.0042	0.0042	0.0059	0.0045	0.0057	0.0060	0.0057	0.0067	0.0076
D	2.27	2.39	2.65	2.56	2.49	2.86	2.14	2.43	2.38	2.22	2.58	2.35
r^2	0.9966	0.9961	0.9936	0.9954	0.9976	0.9922	0.9934	0.9965	0.9967	0.9968	0.9964	0.9978
Modeling T(3/1) vs. Strain												
$T(3/1)_0$ =	15.68	14.13	14.58	14.24	14.34	14.74	14.71	14.75	14.55	14.8	14.78	14.53
α	4.31×10^{-11}	4.47×10^{-11}	3.81×10^{-11}	2.84×10^{-11}	2.84×10^{-11}	3.81×10^{-11}	2.84×10^{-11}	1.77×10^{-11}	1.04×10^{-11}	1.79×10^{-11}	1.44×10^{-11}	6.5×10^{-11}
C	0.0041	0.0051	0.0054	0.0056	0.0057	0.0065	0.0062	0.0064	0.0065	0.0065	0.0070	0.0078
D	2.62	2.99	3.04	3.32	3.34	3.35	2.96	2.91	2.72	2.57	2.76	2.39
R^2	0.9958	0.9951	0.9911	0.9941	0.9962	0.9906	0.9926	0.9965	0.9962	0.9965	0.9964	0.9976

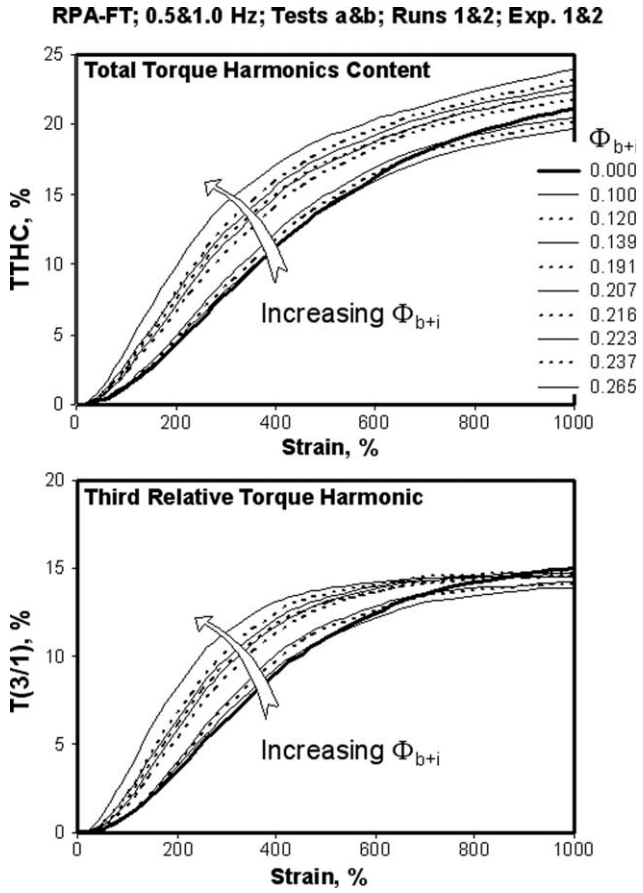

Figure 12 Relative torque harmonics versus strain curves for SBR1500/N330 compounds, as redrawn using eq. (11) and parameters in Table IV.

harmonic T(3/1) and obviously further ones T(5/1), T(7/1), etc. Fit parameters for TTHC and T(3/1) versus strain are given in Table IV.

Fitting data with eq. (11) allows not only to summarize a large number of experimental data in a few relevant parameters but also to derive certain interesting features of the nonlinear viscoelastic behavior of tested materials. For instance Figure 12 compares test results through the fitted curves as redrawn using parameter values given in the table. At first glance a significant difference appears between the third relative harmonic and the overall torque harmonic content. The former clearly reveals the occurrence of a plateau at high strain so that fitting experimental data with the model equation yields so small values for α that $\alpha = 0$ could be considered as well, so that the model reduces to $TH(\gamma) = TH_m \times [1 - \exp(-C\gamma_0)]^D$. However, TTHC versus strain curves do not show (and do not even suggest) the occurrence of a plateau but rather an asymptotic steady increase to a straight line of slope α. This is as expected since would the signal-to-noise ratio be infinite in the Fourier spectrum, one would detect an infinity of odd harmonics that, while smaller and smaller as the harmonic order increases, would nevertheless contribute to an

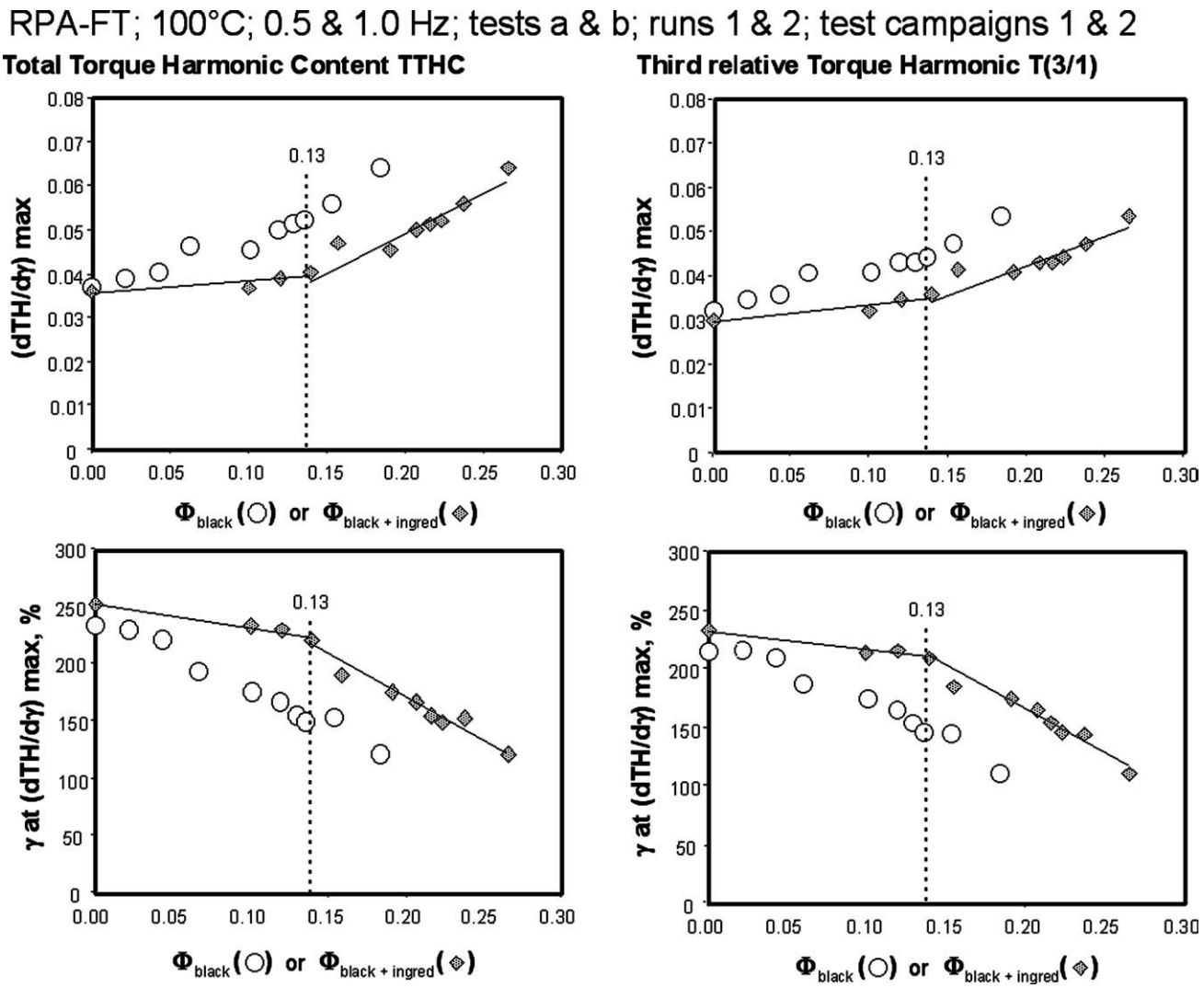

Figure 13 Typical features of torque harmonics variation with SBR formulation; note that the maximum strain sensitivity and the strain for this maximum are plotted either with respect to the sole volume fraction of carbon black or with respect to the overall compounding ingredients volume fraction.

ever increasing TTHC as strain goes to infinity. In practice however, no real material can be infinitely strained and fracture necessarily occurs. Modeling TTHC vs. strain data with eq. (11) allows to well capture this expected behavior.

As seen in Table IV, parameter C tends to increase with filler content but parameter D seems relative insensitive to compounding variations. Mean values $D = 2.39 \pm 0.15$ and $D = 2.88 \pm 0.32$ are calculated respectively for TTHC and $T(3/1)$. First derivative curves are easily calculated with modeling parameters so that a few critical features can be conveniently analyzed. Typical first derivative curves were shown in Figure 11. The maximum first derivative, $\left.\frac{dTH}{d\gamma}\right|_{max}$, is a critical point in the linear-to-nonlinear region that corresponds to the maximum strain sensitivity of the material, and is expectedly affected by compounding ingredients. Figure 13 shows how either the maximum strain sensitivity or the strain amplitude at which this maximum sensitivity is observed varies with formulation. The filler volume fraction or the filler + other ingredients fraction or the solids (i.e., black + ZnO) were considered. As can be seen, when either the carbon black or the solids volume fractions are considered, both $\left.\frac{dTH}{d\gamma}\right|_{max}$ and the strain at $\left.\frac{dTH}{d\gamma}\right|_{max}$ appear to vary in a smooth manner. However when the same data are plotted versus the overall compounding ingredients fraction, then a singularity can be clearly distinguished that corresponds to the (theoretical) percolation level of 0.13–0.14. This means that, as expected, below $\Phi_{b+i} \approx 0.135$ the nonlinear viscoelastic properties of SBR compounds do vary so that mere hydrodynamic effects superimpose to the properties of the polymer matrix. Above this level, filler-filler interactions start to play a significant role so that a nonlinearity of internal origin (i.e., the so-called filler-rubber network) superimposes to the nonlinearity due

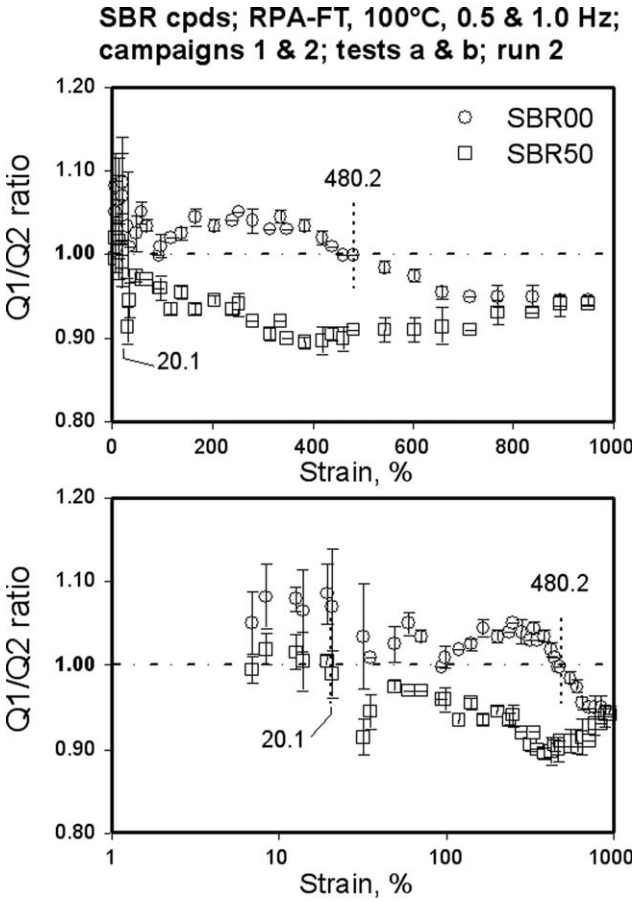

Figure 14 Variation of Q1/Q2 ratio with strain amplitude for the zero black and the 50 phr N330 carbon black compound; averaged data from results at 0.5 and 1.0 Hz; the upper graph uses a linear strain scale; the lower one a log strain scale in order to display the change from an extrinsic to an intrinsic nonlinear viscoelastic behavior.

to large strain amplitude. It is worth underlining that the complex modulus did not permit to clearly detect such effects. The fact that the singularity at the percolation level is clearly seen only if all the compounding ingredients are considered would also suggest that filler-polymer interactions are strongly depending on the minor ingredients of formulation. A plasticizing effect by the "soluble" chemicals, for example, the stearic acid, the oil, and the protective chemicals, of the elastomer fraction in the vicinity of filler particles is a reasonable hypothesis.

The maximum strain sensitivity $\left.\frac{dTH}{d\gamma}\right|_{max}$ is key information about the processing behavior of rubber compounds and the observation that this typical feature of the nonlinear viscoelastic character increases with higher filler (and other ingredients) fraction does correspond well with practical experience on the factory floor. For instance, it is a common observation that the higher the filler loading, the faster the band formation on open mill, with a faster warming-up however. The strain for maximum strain sensitivity conversely decreases with higher filler (and other ingredients) fraction, and does correspond well with the increasing nonlinear character, as already seen through the dynamic strain softening of the complex modulus.

Quarter cycle integration

As demonstrated so far, Fourier Transform rheometry allows clearly quantifying the non-linear response of viscoelastic materials, but experiments with complex polymer systems have revealed that, when submitted to high strain, whether the torque signal is distorted "on the left" or "on the right," with respect to a vertical axis drawn at the first quarter of the cycle, does not reflect in the FT spectrum.[28,32] Most complex polymer systems, for example, filled rubber compounds, exhibit severer distortions, which generally affect more the right part of the half signal, when strong interactions can be suspected between components (i.e., phases) of materials. This difference between the nonlinear viscoelastic behavior of a pure, unfilled polymer, and of a complex polymer material can conveniently by expressed using the terms extrinsic (strain induced, an external effect) and intrinsic (morphology induced, an internal effect) nonlinear viscoelasticity. In order to supplement FT analysis, quarter cycle integration was developed as an easy data treatment technique to distinguish extrinsic and intrinsic nonlinear viscoelasticity. The ratio of the first to second quarters torque signal integration, that is, $Q1/Q2$ allows clearly distinguishing between the strain amplitude effect on a pure (or homogeneous) and a

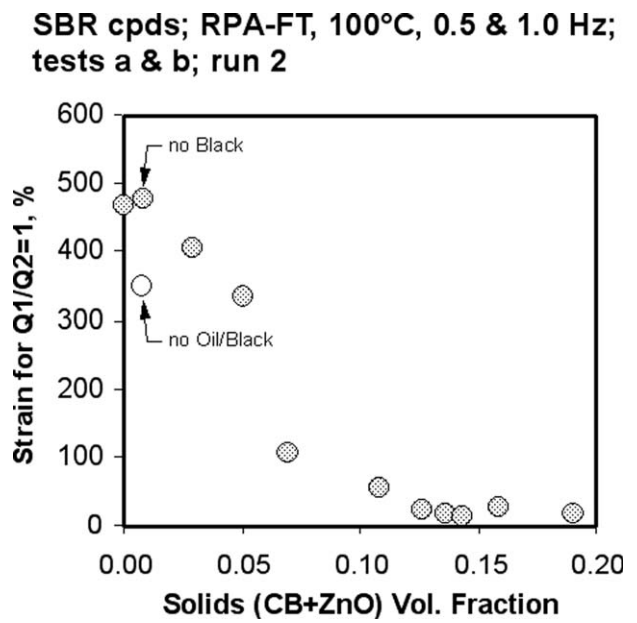

Figure 15 Critical strain for change from extrinsic to intrinsic viscoelastic nonlinearity versus filler (carbon black + zinc oxide) fraction.

complex polymer materials. With the former, $Q1/Q2$ ratio is generally higher than one and is expected to increase with strain amplitude; in such a case the torque signal is always distorted "on the left" (i.e., $Q1 > Q2$). Complex polymer materials generally exhibit $Q1/Q2$ ratio lower than one, which furthermore varies with strain amplitude. This likely reflects changes in interactions between phases that, sometimes, vanish at high strain, thus indicating a profound modification of the compound morphology.

Figure 14 shows how the $Q1/Q2$ ratio varies with strain amplitude for both the zero black and the 50 phr N330 compound. The effect of carbon black is clearly seen as the unfilled compound still exhibits a extrinsic nonlinear viscoelastic behavior up to around 480% strain amplitude, whilst the filled material shows a intrinsic nonlinearity over most of the experimental strain windows. Note that a local Lagragrian interpolation technique was used to assess the strain amplitude for the crossing of $Q1/Q2 = 1$. It is worth underlining that the extrinsic nonlinearity shown by the zero black compound at high strain amplitude was not expected since previously reported results on pure polymers gave always $Q1/Q2$ ratio higher than one.[32] But the gum SBR 1500 sample showed also the same behavior so that it might be conjectured that the (statistically distributed) styrene monomer units do induce an intrinsic nonlinearity appearing only when the strain amplitude is sufficiently large.

The strain amplitude for the $Q1/Q2$ ratio to cross the value 1 (i.e., perfectly symmetry torque signal) is therefore an interesting data that "quantify" the extrinsic/intrinsic nonlinearity. As shown in Figure 15 this critical strain is clearly depending on the filler content, that is, the carbon black and the zinc oxide. One notes also that the oil appears to have an effect. It is worth nothing that a sharp variation seems to occur when the "solids" volume fraction is around 0.04, that is, close to 10 phr carbon black. This value is more than twice lower than the theoretical percolation level and would indicates that, owing to strong interactions between the rubber and the carbon black particles, one does not need *strico sensu* a network of particles throughout the rubber matrix for intrinsic nonlinear viscoelastic effects to appear. It is quite remarkable that a simple torque signal handling technique such as quarter cycle integration gives access to such an information, directly related with the morphology of filled rubber compounds.

CONCLUSIONS

By combining dispersion measurements with results from advanced rheometrical experiments with a closed cavity tester a complete picture emerges as how compounding ingredients do affect the viscoelastic properties of carbon black filled SBR compounds. Linear viscoelastic data are obtained through well-established experimental procedure that consists in probing materials versus frequency at various temperatures in order to obtain mastercurves at a reference temperature. LAOS experiments associated with the capture of torque and strain signals consist in the so-called Fourier transform rheometry, a very fast and accurate technique to investigate the non-linear viscoelastic behavior of polymer materials, particularly complex polymer systems, whose intrinsic nonlinear character severely limits the capabilities of standard harmonic instruments. Adequate strain sweep test protocols lead to reproducible results, particularly in the high strain region, whilst the appropriate data treatment allows minor instruments deficiencies to be compensated for so that results in agreement with theoretical expectations are obtained.

Fourier transform spectra contain all the information available through harmonic testing, and convenient analyses on the nonlinear viscoelastic behavior are made by the variations with strain amplitude of the complex dynamic modulus, of the third relative harmonic and the overall harmonic content torque component $T(3/1)$, and of the torque signal integration. Easy modeling methods give access to various parameters, which clearly reflect the many facets of non-linear viscoelasticity and allows the effects of compounding ingredients to be studied in a very convenient manner. By systematically studying a series of SBR 1500 with carbon black content varying in the 0–50 phr range, it is clearly demonstrated that an essentially nonlinear viscoelastic character arises as soon as the filler content is above 10–15 phr, that is for volume fractions significantly below the theoretical percolation level (13%). It is also seen that the zinc oxide has to be considered as a solid filler whose effect adds to carbon black ones. The other ingredients, namely the processing oil, play essentially a plasticizing role and the mixing has a lower effect than expected.

Interestingly, dispersion measurement results revealed that the lowest carbon black loaded compound has a significantly lower dispersion rating than the zero black one, thus meaning that even minute quantities of black do somewhat penalize the dispersion of other compounding ingredients. Such an observation suits well some of Fourier Transform experiment data. Indeed, it was clearly seen, when analyzing either complex modulus or torque harmonics versus strain data that, as soon as some ingredients, whatever they are, are added to a gum rubber, how the material is responding to mixing stresses is completely changed. Even the smallest carbon black (or any other "solid" ingredient) content does modify how mixing stresses affect the

overall rheological behavior because of specific interactions that develop between such ingredients and the rubber matrix. The mixing energy level plays *per se* a lower role than expected. Such aspects are obviously important would one want to correctly model filled rubber compounds.

References

1. ASTM D3185: Evaluation of SBR (Styrene-Butadiene rubber) including mixtures with oil.
2. Lorenz, C. D.; Ziff, R. M. Phys Rev E 1998, 57, 230.
3. Harter, T. Phys Rev E 2005, 72, 026120.
4. Karasek, L.; Sumita, M. J Mat Sc 1996, 31, 281.
5. Johnson, P. S. In Basic Elastomer technology; Baranwal, K. C., Stephens, H. L., Eds.; The Rubber Division, ACS (2001) – ISBN 091241507x, Chapter 5.
6. Boonstra, B. B. In Rubber Technology, 2nd ed.; Morton, M., Ed.; Van Nostrand Reinhold: New York, 1973; Chapter 3, p 51.
7. Hess, W. M. Rubb Chem Technol 1991, 64, 386.
8. Boonstra, B. B.; Medalia, A. I. Rubb Chem Technol 1962, 36, 115.
9. Vegvari, P. C.; Hess, W. M.; Chirico, V. E. Rubb Chem Technol 1978, 51, 917.
10. Coran, A. Y.; Donnet, J. B Rubb Chem Technol 1992, 65, 973.
11. Persson, S. Polymer Testing 1984, 4, 45.
12. Gerspacher, M.; O'Farrel, C. P. Carbon Black Elastomer Composites Educ. Symp. Nr 49, paper E, 161th Spring Techn. Mtg, Rubber Division, ACS, Savannah, GA, April 2002
13. Leigh-Dugmore, C. H. Rubb Chem Technol 1956, 29, 1303.
14. Medalia, A. I. Rubb Chem Technol 1961, 34, 1134.
15. ASTM D2663. Stantard Test methods for Carbon Black-Dispersion.
16. ISO 11345. Rubber—Assessment of Carbon Black dispersion—Rapid comparative methods.
17. Persson, S. Eur Rubb J 1978, 160, 28.
18. Andersson, L.; Sunder, J.; Persson, S.; Nilsson, L. Rubber World 1999, 219, 36.
19. Putman, J. B.; Putman, M. C.; Samples, R. An improved method for measuring filler dispersion in uncured rubber, paper nr 19, 160th Fall Techn. Mtg., Rubb. Div., ACS, Cleveland, OH, October 2001.
20. Astruc, M. Etude rhéo-optique des mécanismes de dispersion de mélanges sous cisaillement simple: 1. mélanges concentrés de polymères immiscibles, 2. mélanges polymères-charges poreuses, Ph.D. Thesis, Ecoles des Mines de Paris, Sophia-Antipolis, France, October 2001
21. Baranwal, K.; Jacobs, H. L. J Appl Polym Sci 1969, 13, 797.
22. ASTM D6204. Standard Test Method for Rubber – Measurement or unvulcanized rheological properties using rotorless shear rheometer.
23. Leblanc, J. L.; Mongruel, A. Prog Rubb Plast Technol 2001, 17, 162.
24. Debbaut, B.; Burhin, H. J Rheol 2002, 46, 1155.
25. Leblanc, J. L.; de la Chapelle, C. Rubb Chem Technol 2003, 76, 979.
26. Fleury, G.; Schlatter, G.; Muller, R. Rheol Acta 2004, 44, 174.
27. Leblanc, J. L. Rubb Chem Technol 2005, 78, 54.
28. Leblanc, J. L. Rheol Acta 2007, 46, 1013.
29. Wilhelm, M. Macromol Mater Eng 2002, 287, 83.
30. Medalia, A. I. Filler aggregates and their effects on dynamic properties of rubber vulcanizates, Coll. Intern. CNRS, Le Bischenberg, Obernai, France, proceedings, paper #231, 62–79 – Ed. CNRS, Paris (1975) – ISBN 2–222-01749–1, Sept. 1973.
31. Mullins, L.; Tobin, N. R. J Appl Polym Sci 1965, 9, 2993.
32. Leblanc, J. L. J Rubb Res 2007, 10, 63.
33. Leblanc, J. L. J Appl Polym Sci 2008, 109, 1271.
34. Hyun, K.; Wilhelm, M. Macromolecules 2009, 42, 411.